Master's Thesis

Universal quantum computation using a hybrid quantum double model

Katharina Laubscher
July 8, 2017

Department of Physics, University of Basel
Klingelbergstrasse 82, 4056 Basel, Switzerland

Supervisors: Dr. J. R. Wootton
Prof. Dr. D. Loss

Contents

1 Introduction

Quantum systems are inherently sensitive to noise, which severely complicates the physical realization of large scale quantum computers. As a possible solution, quantum error correcting codes have been developed, which in analogy to classical error correcting codes use redundancy to protect logical information. However, the overhead in physical qubits that are needed to encode a single fault-tolerant logical qubit is enormous; additionally, the probabilities with which errors occur have to be sufficiently low in order for error correcting algorithms to succeed. As such, it seems natural to look for alternative approaches to fault-tolerant quantum computation, one of which was found in what is now broadly known as *topological quantum computation*. In its most common form, topological quantum computation is performed using so-called *anyons* in order to store and manipulate logical information. Anyons are exotic particles that arise mathematically in two-dimensional systems. These particles exhibit braiding statistics that are neither fermionic nor bosonic; in fact, the exchange of two identical anyons may in principle realize an arbitrary unitary transformation. As an important feature, a certain class of anyonic models containing so-called *non-Abelian* anyons exhibit non-local degrees of freedom. These give rise to a topologically protected space, which is an ideal place to store quantum information as it is not accessible by perturbations from the environment (which are assumed to act locally). Indeed, it was shown by Kitaev in his famous paper [1] that non-Abelian anyons can be used to store and process quantum information in a way that is intrinsically protected against errors. In particular, he proposed a class of models that could simulate certain anyon models based on a finite group G. These models, known as the $D(G)$ *quantum double models*, feature a two-dimensional spin lattice with qudits placed on each edge. These are locally interacted by a Hamiltonian. The excitations of this system are localized quasiparticles and exhibit anyonic braiding statistics. Later it became evident that even the simpler class of *Abelian* anyon models can be used to perform topological quantum computation if the underlying lattice is suitably modified, which has given rise to the so-called $D(\mathbb{Z}_2)$ surface codes. Both due to their computational power as well as their relative simplicity the $D(\mathbb{Z}_2)$ surface codes have become the most promising approach on the way to universal fault-tolerant quantum computation. There are several ways of encoding quantum information in these codes, e.g. by introducing boundaries to the lattice, by the merging and splitting of separate codes, or by the engineering of defects that show the projective braid statistics of Majorana zero modes. The ways to fault-tolerantly perform Clifford operations for each encoding, and even combinations of different encoding schemes, have extensively been studied. The standard way to achieve universal quantum computation with these schemes is the distillation and injection of so-called *magic states*. In this thesis we discuss an alternative approach to complement the gate set of the $D(\mathbb{Z}_2)$ surface codes such that universal quantum computation can be achieved. We consider a planar code that is divided into two half-planes, where one half-plane is associated with the $D(\mathbb{Z}_2)$ quantum double model and the other one with the $D(S_3)$ quantum double model. We are going to call such models *hybrid quantum double models*. We propose a procedure that allows us to prepare non-stabilizer states in the $D(S_3)$ phase and then inject these states into the $D(\mathbb{Z}_2)$ phase, where they can be used to complete the gate set that can be realized from standard

$D(\mathbb{Z}_2)$ surface code computational schemes.

This thesis is organized as follows. The first part consists of a review of the most important concepts that are needed in order to understand and use Kitaev's quantum double model construction in the context of topological quantum computation: In Sec. 2 we briefly introduce the basic concepts of anyon models and topological quantum computation. Sec. 3 gives a short summary of the mathematical construction of the anyon models emerging from discrete gauge theories based on a finite group G. In Sec. 4 we introduce Kitaev's $D(G)$ quantum double models in order to simulate these anyon models on an infinite two-dimensional spin lattice, and Sec. 5 extends this construction to the case of a lattice with boundaries. We also introduce the more general concept of domain walls between regions of the lattice associated with different quantum double models. In Sec. 6 we discuss the realization of suitable stabilizer circuits for arbitrary quantum double models similar to the ones used in the $D(\mathbb{Z}_2)$ surface codes. The knowledge that was built up in these first few sections is then applied in the second part of this thesis. We start by briefly reviewing the $D(\mathbb{Z}_2)$ and the $D(S_3)$ quantum double models in their own right in Secs. 7 and 8, respectively. Sec. 9 then comprises the core of this work, where we present a way to perform universal quantum computation using a hybrid quantum double model consisting of a lattice divided into two half-planes, where one half-plane is associated with the $D(\mathbb{Z}_2)$ quantum double model and the other one with the $D(S_3)$ quantum double model. Logical information is stored in the $D(\mathbb{Z}_2)$ part of the lattice using the usual hole-pair encoding, for which we perform initialization processes, measurements and the full set of Clifford operations using the standard procedures. We then use our knowledge of the braiding rules of the $D(S_3)$ quantum double model to prepare a non-stabilizer state in the $D(S_3)$ part of the lattice, and propose a protocol to inject such a state state into the $D(\mathbb{Z}_2)$ phase. This allows us to perform universal quantum computation in the $D(\mathbb{Z}_2)$ part of the lattice, replacing the standard magic state distillation procedures by the injection of a non-stabilizer state from a foreign phase. We also discuss the reverse process, i.e. the transport of logical information from the $D(\mathbb{Z}_2)$ phase to the $D(S_3)$ phase. This enables us to manipulate logical information in the $D(S_3)$ part of the lattice, further enlarging the set of possible operations and providing even more flexibility. Finally, we give a few concluding remarks in Sec. 10.

Throughout this work we assume that the reader is familiar with the concepts of quantum computation, an excellent introduction to which can be found in the standard textbook by Nielsen and Chuang [2]. Furthermore, we require a basic knowledge of group theory and in particular of the representation theory of finite groups. Knowledge of the $D(\mathbb{Z}_2)$ surface codes is helpful but not explicitly necessary; all the required information can be found following the corresponding references.

2 Preliminaries

In this section we introduce some of the basic concepts and notations that are used throughout this work. In Sec. 2.1 we briefly review the abstract description of anyon models, and in Sec. 2.2 we introduce the concept of topological quantum computation with anyons.

2.1 The theory of anyons

In three dimensions, the exchange statistics of identical particles can easily be described. If the particles are bosons, the wave function of a many-particle state remains unchanged upon the exchange of two particles, whereas if the particles are fermions, the wave function acquires a global phase factor of -1. In two dimensions the possible exchange statistics are remarkably richer. There exist particles which are neither bosons nor fermions, and are therefore called *anyons* (deduced from *'any'-ons*). Exchanging two anyons may result in an arbitrary phase factor $e^{i\phi}$ in the case of Abelian anyons, or even in a higher-dimensional unitary transformation in the case of non-Abelian anyons. The following introduction focuses on the most basic properties of anyons and serves as a platform to introduce the notations that are going to be used in this context throughout this work. For excellent introductions to anyon theory see for example Refs. [3, 4].

In order to specify an anyon model, we start with a list of the constituent particles. Every anyon model contains the vacuum as a particle, i.e. the absence of a particle is considered to be a special type of particle. Often the vacuum particle will be denoted by the number 1, whereas we will mostly use letters, latin or greek, in order to label the non-trivial particle types. Furthermore, we need to specify how two anyons behave collectively when they are brought together. This process is called *fusion* of the particles and will be denoted by '$\times$'. The required information is given by the so-called *fusion rules* of the model, which take the general form

$$a \times b = \sum_c N_{ab}^c \; c \tag{2.1}$$

for two anyons labelled a and b and with the sum running over all particles of the corresponding anyon model. The *fusion multiplicities* N_{ab}^c are non-negative integers and count the distinguishable ways in which the anyons a and b can fuse to yield the anyon c. If $N_{ab}^c = 0$ for a certain anyon c, then it is impossible for a and b to fuse to c. The sum is thus to be understood as listing the different possible fusion outcomes, or *fusion channels*, of a and b. The fusion rules are associative and commutative, and the vacuum particle 1 acts as the identity element of the fusion operation, i.e. $1 \times a = a \times 1 = a$ for all anyons a of the model. Furthermore, there needs to exist an antiparticle $\bar{a}$ for each anyon a such that $a \times \bar{a}$ has the vacuum as a possible fusion outcome. Fusion rules can also be time-reversed and interpreted as decay rules; in particular this means that it is possible to create particle-antiparticle pairs $a, \bar{a}$ from the vacuum. It is important to note that for two anyons a, b their fusion outcome is a non-local property in the sense that it can neither be attributed to a or to b, and can in general only be determined by explicitly bringing the two anyons together and observing their properties as a composite particle.

If we consider a collection of multiple anyons, we can fuse them one by one in order to obtain a single anyon. We can now look at the distinguishable ways in which they can fuse to a certain anyon while keeping the order of subsequent fusion processes fixed. These are given by different intermediate fusion outcomes, and the corresponding states constitute a basis of the so-called *fusion space* of the collection of anyons. Fusing the anyons in a different order corresponds to choosing a different basis for the same fusion space. The simplest example of such a process is the case of three anyons a, b, c that fuse to an anyon d. Fusing a and b first may result in different possible fusion outcomes $e_1, e_2, ..., e_n$ which then yield d upon fusion with c. The different intermediate outcomes $\{e_i | i = 1, ..., n\}$ label the basis states of the fusion space. In the following chapters we are going to denote these states by $|a, b \to e_i\rangle$ for $i = 1, ..., n$. If a and b are clear from context, we sometimes also just write $|e_i\rangle$ instead of $|a, b \to e_i\rangle$. If we had fused the anyons b and c first, the intermediate fusion outcomes would specify a different set of basis states $\{|b, c \to e'_i\rangle | i = 1, ..., n\}$. The so-called F *matrices* describe the corresponding changes of basis by relating the different possible fusion orders of a collection of three anyons. The definition of the F operation is visualized in Fig. 2.1(a). Basis states for fusion spaces of larger collections of anyons are labelled by multiple intermediate fusion outcomes, and the corresponding changes of basis can be constructed from multiple F operations acting on suitable subsets of the collection.

According to their fusion rules we can classify anyons in two families: For *Abelian* anyons all fusion processes have a definite outcome, i.e. the fusion rules take the form

$$a \times b = c \tag{2.2}$$

for all anyons a, b of the model. For a *non-Abelian* anyon model, however, different possible fusion outcomes as well as fusion multiplicities higher than one are allowed. It is easy to see from Eq. (2.2) that the fusion space of an arbitrary collection of Abelian anyons is always trivial. In the case of non-Abelian anyons, however, the corresponding fusion space can be of arbitrary dimension. We can operate on the fusion space by *braiding* the constituent anyons, i.e. by permuting their positions. The effect of braiding two anyons a and b with a definite fusion outcome c yields a complex phase factor which is denoted R^c_{ab}. A pictorial representation of this braiding operation can be found in Fig. 2.1(b). By ordering the phase factors for all the different fusion channels of a and b on the diagonal of a matrix we obtain the *braiding matrix* or R *matrix* R_{ab}. Exchanging two non-Abelian anyons a and b which are in a superposition of different fusion channels performs a unitary transformation B_{ab} on the corresponding fusion space, which can be calculated by first changing into the basis where their fusion outcome is definite, applying R_{ab} and finally performing the inverse change of basis. To make this explicit, consider three anyons a, b, c with fusion outcome d such that b and c fuse to e'. The exchange of a and b then results in the transformation

$$B_{ab} = (F^b_{acd})^{-1} R_{ab} F^b_{acd}, \tag{2.3}$$

which is non-diagonal in general. From a more abstract point of view, if we assume that we have n anyons arranged in a line indexed by their corresponding position on that line, the set of all possible exchanges of neighbouring anyons B_{ij} for $i = j \pm 1$ generates a matrix representation of the so-called *braid group*

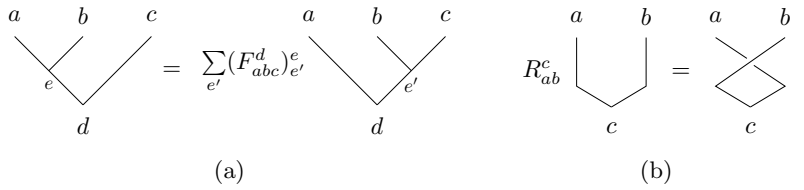

(a) (b)

Figure 2.1: (a) The matrix F^d_{abc} implements a change of basis on the fusion space of three anyons a, b, c with fusion outcome d by relating the different possible intermediate fusion outcomes for one fusion order to the intermediate fusion outcomes for a different fusion order. In this diagrammatic notation the index e denotes a certain fusion outcome of a and b, while the sum runs over all possible fusion outcomes e' of b and c. (b) The matrix R^c_{ab} realizes the clockwise exchange of two anyons a and b with fusion outcome c.

which is carried by these of anyons. By studying this representation for different collections of anyons, the set of gates which can be realized by braiding in a certain anyon model can be determined.

Given a set of particles, the corresponding F and R matrices have to satisfy certain consistency relations. In fact, it turns out that there are exactly two sets of equations that have to be satisfied by all of the F and R matrices such that they specify a consistent anyon model. These are known as the *Pentagon equations* and the *Hexagon equations*. However, we are not going to discuss these equations here. Instead we proceed to give a short summary on how anyons can be used for quantum computation.

2.2 Topological quantum computation

Topological quantum computation uses non-local degrees of freedom to store quantum information. In particular, quantum information can be encoded in the fusion space of a collection of non-Abelian anyons by identifying the computational basis of a qudit with d orthogonal fusion channels of this collection. Logical gates are performed by braiding the constituent anyons. If the transformations that can be implemented by braiding generate a dense set of unitaries acting on these qudits, the corresponding model is universal for quantum computation in the sense that any unitary transformation can be approximated arbitrarily well by braiding operations. The most famous example of an anyon model that is universal by braiding are the so-called *Fibonacci anyons* [5]. As described in the previous subsection, the fusion space cannot be accessed by local operations on single anyons, nor can it be accessed by LOCC[1] protocols, as long as all the particles are kept far apart from each other. Thus, the encoded information is intrinsically protected from local perturbations. This is the fault-tolerant characteristic of anyons that makes them a favourable medium for performing quantum computation. Furthermore, the unitary transformations induced by the braiding of anyons do not depend on the exact paths spanned by the anyons, only on their topology. This makes these operations indifferent to small perturbations from the environment.

Apart from the fusion space encoding, there are other (though related) approaches to topological quantum computation, some of which we are going to

[1] *L*ocal *O*perations and *C*lassical *C*ommunication

encounter in the following sections of this work. Interestingly, some of these schemes allow it to perform topological quantum computation even with Abelian anyons.

3 Anyons from discrete gauge theories

In this chapter we introduce the algebraic construction of a certain class of anyon models. The corresponding mathematical theory has its origin in the field of topological quantum field theory, an introduction to which would be beyond the scope of this work. In general, one starts with a Lagrangian that is invariant under a continuous symmetry group H. The Lagrangian involves a Higgs field, which may be coupled to some external matter fields. By spontaneous symmetry breaking, the global symmetry group H is reduced to a finite subgroup G of H. The broken phase supports topological defects, which can be classified by quantum numbers that are invariant under all residual gauge transformations from H. In the following we focus on characterizing the emerging anyon models within the framework that was introduced in the previous section. For a rigorous mathematical treatment of discrete gauge theories the reader is referred to the original papers [6–8], and a pedagogical introduction for physicists can be found in Ref. [9].

Let G be a finite group. Throughout this work we denote the identity element of G by 1 unless stated otherwise. We denote the set of conjugancy classes of G by $(G)_{\text{conj}}$, and for the conjugancy class corresponding to a given representative $r_C \in C$ we will write C_{r_C}. Furthermore, we label the centralizer of an element $g \in G$ by N_g. Recall that the definition of the centralizer is $N_g = \{h \in G | gh = hg\}$. Let us denote the set of unitary irreducible representations of G by $(G)_{\text{irrep}}$. However, as for a finite group G every irreducible representation is equivalent to a unitary irreducible representation, we are not going to mention the unitarity explicitly for the rest of this work. The anyons in the spectrum of the discrete gauge theory based on the finite group G are then labelled as follows: Each particle is given by a conjugancy class $C \in (G)_{\text{conj}}$ and an irreducible representation $R \in (N_{r_C})_{\text{irrep}}$ for a representative $r_C \in C$. Note that the choice of fiducial element for the conjugancy class C is arbitrary in this context, as N_{r_C} is isomorphic to $N_{r'_C}$ for two representatives $r_C, r'_C \in C$. As such we are going to label the centralizer only by the conjugancy class and write N_C instead of N_{r_C} from now on. For historical reasons the elements that correspond to a given conjugancy class C and the trivial representation of N_C are called *magnetic fluxes*, whereas the particles corresponding to the trivial conjugancy class C_1 and an irreducible representation of $N_{C_1} = G$ are called *electric charges*. In general a particle corresponds to a combination of those two types; such particles are called *dyons*.

Given the particle types of an anyon model, we need to specify their fusion and braiding rules. In order to describe these rules, let us first introduce a more elegant characterisation of the anyon types of the model. For a finite group G, consider the group algebra $\mathbb{C}[G]$ as the space of formal linear combinations of group elements with complex coefficients. The multiplication inherited from G makes $\mathbb{C}[G]$ an algebra. We can interpret $\mathbb{C}[G]$ as a complex Hilbert space by introducing the orthonormal basis $\{|g\rangle | g \in G\}$. Furthermore, consider the dual space $\mathcal{F}(G) = \{f : G \to \mathbb{C}\}$. We introduce an orthonormal basis for $\mathcal{F}(G)$

given by the set $\{P_h|h \in G\}$ with P_h being the projection onto a group element $h \in G$, i.e. $P_h = |h\rangle\langle h|$. $\mathcal{F}(G)$ is an algebra with the multiplication

$$P_h P_{h'} = \delta_{h,h'} P_h. \tag{3.1}$$

We then define the *quantum double* $D(G)$ of G as the algebra generated by the elements

$$\{P_h g|h, g \in G\}. \tag{3.2}$$

The generating elements satisfy the commutation rule

$$gP_h = P_{ghg^{-1}} g, \tag{3.3}$$

which can be combined with the multiplication rules of the group algebra $\mathbb{C}[G]$ and its dual algebra $\mathcal{F}(G)$ in order to give the multiplication rule for the quantum double,

$$P_h g P_{h'} g' = \delta_{h,gh'g^{-1}} P_h g g'. \tag{3.4}$$

The construction of $D(G)$ was introduced by Drinfeld in Ref. [10] and is therefore sometimes called the *Drinfeld double*. Actually $D(G)$ is not only an algebra but a quasitriangular Hopf-algebra, but we are not going to use a lot of its additional structure here. The quantum double $D(G)$ for a finite group G allows a particularly elegant description of the particle spectrum of the discrete gauge theory based on the group G. Let us label the elements for each $C \in (G)_{\text{conj}}$ by $C = \{h_1^C, ..., h_{|C|}^C\}$. We let $N_C = N_{h_1}$ and fix a basis for the representation space of each $R \in (N_C)_{\text{irrep}}$ and label the basis states as $\{|v_1^R\rangle, ..., |v_{n_R}^R\rangle\}$, where we have used n_R to denote the dimension of the representation R. Then each particle carries an internal Hilbert space which is spanned by the basis states

$$\{|h_i^C, v_j^R\rangle | i \in \{1, ..., |C|\}, j \in \{1, ..., n_R\}\}. \tag{3.5}$$

It turns out that the irreducible representations of $D(G)$ are in one-to-one correspondence with the set of particles given by $\{(R, C)|C \in (G)_{\text{conj}},\ R \in (N_C)_{\text{irrep}}\}$, as can be seen by the following construction: Let us denote a set of representatives for each equivalence class in G/N_C by $Q^C = \{q_1^C, ..., q_{|C|}^C\}$ such that $h_i^C = q_i^C h_1^C (q_i^C)^{-1}$. We will always choose $q_1^C = e$. Then the action of an element $P_h g \in D(G)$ on a basis state from the set (3.5) is given by

$$\Pi_R^C(P_h g)|h_i^C v_j^R\rangle = \delta_{h,gh_i^C g^{-1}} \sum_l |g h_i^C g^{-1}, R(\hat{g})_{lj} v_l^R\rangle, \tag{3.6}$$

where

$$\hat{g} = (q_k^C)^{-1} g q_i^C \tag{3.7}$$

with k defined such that $h_k^C = g h_i^C g^{-1}$. One can check that $\hat{g}$ indeed commutes with h_1^C and therefore is an element of N_C. This action of $D(G)$ is irreducible, and conversely every irreducible action of $D(G)$ is of this form. Thus we can index the irreducible representations of $D(G)$ by pairs (R, C), where $C \in (G)_{\text{conj}}$ and $R \in (N_C)_{\text{irrep}}$. In the following chapters we are going to denote an arbitrary representation of $D(G)$ by Π_R^C and the corresponding particle by (R, C), implicitly requiring R and C to be of the form that was specified above.

The Hopf algebra structure of $D(G)$ also provides us with a so-called *comultiplication* $D(G) \to D(G) \times D(G)$, $P_h g \mapsto \Delta(P_h g)$ given by

$$\Delta(P_h g) = \sum_{h'h''=h} P_{h'} g \otimes P_{h''} g. \tag{3.8}$$

The comultiplication allows us to extend the action of the quantum double from one-particle states to two-particle states. This action can be understood in the following way: The residual global symmetry transformations $g \in G$ affect the internal states of the two particles separately. The projection operator P_h subsequently projects out the total flux of the two-particle state, i.e. the product of the two fluxes. Hence, this action of the quantum double determines the global properties of a given two-particle state which are conserved under the process of fusing the two particles. As such, two particles given by (R', C'), (R'', C'') also correspond to a representation of $D(G)$, with the tensor product representation of $D(G)$ on the two-particle state being defined as $\Pi^{C'}_{R'} \otimes \Pi^{C''}_{R''}(\Delta(P_h g))$. However, this representation is not irreducible in general. If the two particles are fused, and thus turned into a single particle, the possible fusion outcomes are given by the decomposition of this representation into irreducible components

$$\Pi^{C'}_{R'} \otimes \Pi^{C''}_{R''} = \bigoplus_{\Pi^C_R} N^{CC'C''}_{RR'R''}\ \Pi^C_R. \tag{3.9}$$

Here Π^C_R runs over all irreducible representations of $D(G)$ and $N^{CC'C''}_{RR'R''}$ corresponds to the multiplicity of the representation Π^C_R. From a general group-theoretical argument it can be inferred that $N^{CC'C''}_{RR'R''}$ is given by

$$N^{CC'C''}_{RR'R''} = \frac{1}{|G|} \sum_{h,g} \mathrm{tr}\{\Pi^{C'}_{R'} \otimes \Pi^{C''}_{R''}(\Delta(P_h g))\}\ \mathrm{tr}\{\Pi^C_R(P_h g)\}^*. \tag{3.10}$$

This specifies the fusion rules (2.1) in the explicit case of the anyon models emerging from discrete gauge theories. The braiding operation that acts on a two-particle state as the counterclockwise exchange of the two particles is given by

$$\mathcal{R}^{C'C''}_{R'R''} = \sigma \circ\ (\Pi^{C'}_{R'} \otimes \Pi^{C''}_{R''})(B), \tag{3.11}$$

where B is the so-called *formal braiding operation*,

$$B = \sum_{h,g} P_g \otimes P_h g \in D(G) \otimes D(G). \tag{3.12}$$

The consistency of this braiding operation with the fusion rules discussed above is guaranteed by the quasitriangularity of $D(G)$. Arbitrary as its definition may seem, we can gain a lot of intuition by considering the explicit action of the braiding operation on a two-particle state in terms of the basis states (3.5). For two basis states $|h^{C'}_i, v^{R'}_j\rangle \otimes |h^{C''}_k, v^{R''}_l\rangle \in V^{C'}_{R'} \otimes V^{C''}_{R''}$ we can write the action of the braiding operation as follows:

$$\begin{aligned} &\mathcal{R}^{C'C''}_{R'R''} |h^{C'}_i, v^{R'}_j\rangle \otimes |h^{C''}_k, v^{R''}_l\rangle \\ &\qquad = |h^{C'}_i h^{C''}_k (h^{C'}_i)^{-1}, \sum_m R''(\hat{h}^{C'}_i)_{ml} v^{R''}_m\rangle \otimes |h^{C'}_i, v^{R'}_j\rangle, \end{aligned} \tag{3.13}$$

with $\hat{h}_i^{C'}$ defined according to Eq. (3.7). In the case of two pure fluxes $(\mathbb{1}, C')$, $(\mathbb{1}, C'')$, where we have used $\mathbb{1}$ to denote the trivial representation of G, this simplifies to

$$\mathcal{R}_{\mathbb{1}\ \mathbb{1}}^{C'C''}|h_i^{C'}, v_1^{R'}\rangle \otimes |h_k^{C''}, v_1^{R''}\rangle = |h_i^{C'} h_k^{C''} (h_i^{C'})^{-1}, v_1^{R''}\rangle \otimes |h_i^{C'}, v_1^{R'}\rangle, \quad (3.14)$$

which is called the *flux metamorphosis*. Its effect is simply given by a conjugation of the flux of the second particle by the flux of the first particle and a permutation of the particles. Similarly, one can also consider the braiding operation (3.13) in the case of a pure flux $(\mathbb{1}, C')$ and a pure charge (R', C_1), where we have used C_1 to denote the conjugancy class corresponding to the identity element:

$$\mathcal{R}_{\mathbb{1}\ R''}^{C'C_1}|h_i^{C'}, v_1^{\mathbb{1}}\rangle \otimes |h_1^{C_1}, v_l^{R''}\rangle = \sum_m |h_1^{C_1}, R''(h_i^{C'})_{ml} v_m^{R''}\rangle \otimes |h_i^{C'}, v_1^{\mathbb{1}}\rangle. \quad (3.15)$$

This corresponds to applying the gauge transformation given by the flux $h_i^{C'}$ of the first particle in the representation R'' to the charge state $|v_l^{R''}\rangle$ of the second particle. This effect is called the generalized Aharonov-Bohm effect in analogy to the effect which is usually called the (Abelian) Aharonov-Bohm effect in basic quantum mechanics, where an electrically charged particle gains an additional phase factor when it encircles a magnetic flux line. These two special cases of the braiding operation, the flux metamorphosis and the Aharonov-Bohm effect, can be considered the main building blocks of anyonic quantum computational gates that are performed by anyon braiding in these models. They should always be kept in mind during the next few sections. Note that braiding two pure charges acts trivially, as can be seen by explicitly writing out the corresponding effect of the braiding operation on two basis states in the same way as above. When we are dealing with dyons, the general braiding rule given by Eq. (3.13) has to be employed.

Note that it is possible to obtain explicit expressions for the states corresponding to the different fusion channels of two or more anyons in terms of the internal basis states (3.5) by considering the action of the quantum double on the composite state via the definition of the comultiplication that was given in Eq. (3.8). In particular, the linear combination of internal basis states corresponding to the vacuum fusion channel can be obtained by requiring that the composite state i) has trivial total flux and ii) transforms trivially under the action of every gauge transformation $g \in G$. As an illustration, let us consider a two-particle state consisting of two pure fluxes $(\mathbb{1}, C')$, $(\mathbb{1}, C'')$ in the vacuum fusion channel. The trivial total flux condition implies that the flux labelling the corresponding internal states has to multiply to the identity element 1 of the group G. In particular, this means $C'' = \bar{C}'$, where we use $\bar{C}$ to denote the inverse conjugancy class of a conjugancy class C. The second condition requires that the superposition has to include all internal basis states with equal weight. We thus get the following expression for the particle-antiparticle pair $(\mathbb{1}, C)$ and $(\mathbb{1}, \bar{C})$ in the vacuum fusion channel:

$$|\mathrm{Vac}_C\rangle = \frac{1}{\sqrt{|C|}} \sum_{i=1}^{|C|} |c_i\rangle \otimes |c_i^{-1}\rangle. \quad (3.16)$$

Similarly, for a pair of pure charges (R', C_1), (R'', C_1) in the vacuum fusion channel the internal basis states have to transform under conjugate irreducible

representations, which in particular implies $R'' = (R')^*$ with R^* labelling the conjugate representation of a representation R. Furthermore, the superposition has to contain all internal basis states with equal weight. The state of the particle-antiparticle pair (R, C_1), (R^*, C_1) in the vacuum fusion channel can thus be expressed as

$$|\mathrm{Vac}_R\rangle = \frac{1}{\sqrt{n_R}} \sum_{j=1}^{n_R} |v_j\rangle \otimes |v_j^*\rangle, \tag{3.17}$$

with $|v_j\rangle$ labelling the basis states of the representation R' and $|v_j^*\rangle$ labelling the corresponding basis states of the conjugate representation R'^*. By combining the above arguments, similar rules for the vacuum fusion channel of dyonic combinations can be obtained. Furthermore, it is also possible to analyse other fusion channels by first determining how the composite state should transform under the action of the quantum double and then looking for the superposition of internal states that satisfies these conditions. This is going to give us a lot of insight in the next section, when we analyse a specific model that realizes anyon models emerging from discrete gauge theories and are interested in using different fusion channels of certain anyons to store quantum information.

4 Kitaev's quantum double models

In the following subsections we introduce a construction that simulates the anyon models described in the last section as localized excitations on a two-dimensional spin lattice. These models are called the *quantum double models* and were proposed by Kitaev in 1997 in Ref. [1]. They use highly entangled states in order to realize the non-local properties of anyon models. The braiding of anyons is realized by explicitly moving the quasiparticles around the lattice, and full monodromies can be shown to yield the same effect as predicted by the general theory. However, this is not always true for single exchanges. Furthermore, there are additional local degrees of freedom associated with each anyon that do not appear in the abstract theory presented in Sec. 3. While these degrees of freedom are not affected by braiding, other operations like fusion may well cause rotations in these internal spaces. When designing schemes for quantum computation it is therefore important that at no point it is possible for information to leak out of the topologically protected space into these local subspaces. In Sec. 4.1 we review the general construction of the quantum double models on a spin lattice, and in Sec. 4.2 we discuss the operators that are needed to explicitly create, move, fuse and detect anyonic quasiparticles in these models. Sec. 4.3 finally tries to give an intuitive picture of the fusion and braiding of quasiparticles in this model. While we do not hesitate to introduce certain formal expressions and arguments where they are considered to help the general understanding of the model, most of the higher mathematical background of the theory is omitted in order to make this work accessible to a broader audience.

4.1 General construction

A suitable model to simulate the particle spectrum of the anyon models introduced in Sec. 3 was proposed by Kitaev in Ref. [1]. His construction features a

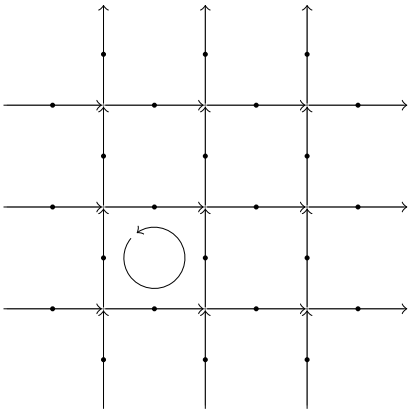

Figure 4.1: We consider a square lattice with $|G|$-level spins, shown as dots, placed on each edge. Each edge has an orientation that is indicated by an arrow. Furthermore, we choose an orientation for every plaquette, as is shown here by a circled arrow for one specific plaquette. In our case, all the plaquettes are oriented counterclockwise.

lattice where $|G|$-level spins, or in other words qudits with $d = |G|$, are placed on each edge, see Fig. 4.1. For simplicity we focus on a square lattice on an infinite plane, even though the original construction works for an arbitrary lattice on any orientable two-dimensional surface. As introduced earlier let $\mathbb{C}[G]$ denote the complex group algebra corresponding to G, for which we again fix the orthonormal basis $\{|g\rangle | g \in G\}$. The spins at the edges of the lattice take values in $\mathbb{C}[G]$ such that the total Hilbert space of the system is $\otimes_e \mathbb{C}[G]$. Now we define operators acting on a state $|a\rangle$ for $a \in G$ corresponding to the left and right multiplication by a given group element $g \in G$,

$$L_+^g |a\rangle = |ga\rangle, \quad L_-^g |a\rangle = |ag^{-1}\rangle, \tag{4.1}$$

and we extend their action to the whole group algebra $\mathbb{C}[G]$ by linearity. Moreover we define projectors onto basis states $|h\rangle \in G$,

$$P_+^h |a\rangle = \delta_{h,a}|a\rangle, \quad P_-^h |a\rangle = \delta_{h^{-1},a}|a\rangle. \tag{4.2}$$

Again we extend their action on an arbitrary element of the group algebra by linearity. Here, $\delta_{i,j}$ denotes the Kronecker delta function. The operators (4.1) and (4.2) satisfy the commutation relations

$$L_+^g P_+^h = P_+^{gh} L_+^g, \tag{4.3}$$

$$L_+^g P_-^h = P_-^{hg^{-1}} L_+^g, \tag{4.4}$$

$$L_-^g P_+^h = P_+^{hg^{-1}} L_-^g, \tag{4.5}$$

$$L_-^g P_-^h = P_-^{gh} L_-^g. \tag{4.6}$$

We choose a specific orientation for each edge as well as for each plaquette of the lattice as is indicated by arrows in Fig. 4.1. Note that this orientation is a matter of choice; reversing the orientation of an edge corresponds to relabelling the basis elements for the corresponding spin from $|g\rangle$ to $|g^{-1}\rangle$. Let us now fix some notations. For a spin j we write e_j to denote the corresponding edge

of the lattice. For two vertices v, v' we use the notation $[v, v']$ to denote the edge which points from v to v'. Moreover, let $\mathrm{star}(v)$ denote all edges that are connected to the vertex v. We write $[*, v] \subset \mathrm{star}(v)$ for the set of edges that are incident on v, and $[v, *] \subset \mathrm{star}(v)$ for the set of outgoing edges of v. For a plaquette p we write ∂p to denote the set of edges spanning the boundary of the plaquette p. $[p, +] \subset \partial p$ is used to denote the set of edges that have the same orientation as p, and $[p, -] \subset \partial p$ denotes the set of edges that have opposite orientation to p. We proceed to define the following operator acting on a single spin j with $e_j \in \mathrm{star}(v)$:

$$L^g(e_j, v) = \begin{cases} L^g_+(j) & e_j \in [*, v] \\ L^g_-(j) & e_j \in [v, *] \end{cases} . \tag{4.7}$$

This operator acts on the spin j as a left or right multiplication by g, depending on the orientation of the edge e_j with respect to the vertex v. Furthermore, let us define the operator

$$P^h(e_j, p) = \begin{cases} P^h_+(j) & e_j \in [p, -] \\ P^h_-(j) & e_j \in [p, +] \end{cases} \tag{4.8}$$

acting on a single spin j with $e_j \in \partial p$. This corresponds to projecting the state of the spin j onto either h or its inverse, depending on the orientation of the edge e_j with respect to the plaquette p.

These operators are now used to define 4-body operators acting on the 4 spins adjacent to each vertex and on the 4 spins on the boundary of each plaquette as follows:

$$A^g(v) = \prod_{e_j \in \mathrm{star}(v)} L^g(e_j, v), \tag{4.9}$$

$$B^h(p, v) = \sum_{\substack{\prod_{e_j \in \partial p} h_j = h \\ e_0 \in \mathrm{star}(v) \\ \text{counterclockwise}}} \prod_{e_j \in \partial p} P^{h_j}(e_j, p). \tag{4.10}$$

$A^g(v)$ acts on the 4 spins surrounding the vertex v by left or right multiplication with g, depending on the orientation of the corresponding edge. $B^h(p, v)$ projects out the states for which the product of group elements along the boundary of p is h, starting and ending at vertex v and proceeding in counterclockwise order. In Fig. 4.2(a) the effect of these operators is visualized in a graphical way. Note that $A^g(v)$ only depends on v, whereas $B^h(p, v)$ indeed depends on both p and v unless h is a central element of G. Nevertheless, we are going to refer to the operators A^g_v as the vertex operators and to the operators B^h_p as the plaquette operators, keeping in mind that the latter implicitly depend on a vertex as well. Finally, let us define the following operators for each plaquette p and each vertex v, respectively:

$$B(p) = B^1(p, v), \tag{4.11}$$

$$A(v) = \frac{1}{|G|} \sum_{g \in G} A^g(v). \tag{4.12}$$

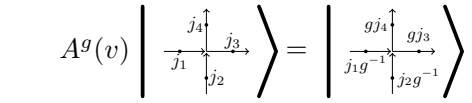

(a)

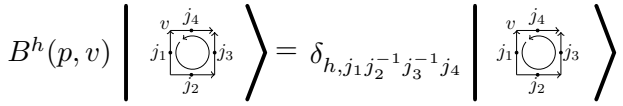

(b)

Figure 4.2: (a) $A^g(v)$ acts on the 4 qubits surrounding the vertex v by left or right multiplication by g, depending on the orientation of the corresponding edge. (b) $B^h(p,v)$ projects out the states for which the product of group elements along the boundary of p is h, starting and ending at vertex v and proceeding in counterclockwise order.

$B(p)$ only depends on p and $A(v)$ only depends on v. Both are projectors and they commute pairwise, i.e. $[A(v), B(p)] = 0\ \forall v, p$, which can be verified using the commutation relations given in Eqs. (4.3)-(4.6). Additionally we have $[A_v, A_{v'}] = 0\ \forall v, v'$ due to the orientation of the lattice, and trivially $[B_p, B_{p'}] = 0\ \forall p, p'$. This now allows us to define the Hamiltonian

$$H^G = -\sum_v A(v) - \sum_p B(p), \tag{4.13}$$

where the sums run over all vertices and all plaquettes of the lattice, respectively. In order to establish a clear notation for the following sections, where multiple quantum double models based on different groups might be involved at the same time, we label the Hamiltonian by the corresponding group G. The ground state $|GS\rangle$ of H^G is the simultaneous $+1$ eigenspace of all the vertex operators as well as all the plaquette projectors,

$$A(v)|GS\rangle = |GS\rangle, \quad B(p)|GS\rangle = |GS\rangle \quad \forall\ v, p\ . \tag{4.14}$$

We say that the operators $A(v)$ and $B(p)$ *stabilize* the ground state and we call them the vertex and plaquette *stabilizers*. In fact, the $D(\mathbb{Z}_2)$ quantum double model is an example of a stabilizer code according to its original definition as given in Ref. [11], and the other quantum double models can be viewed as generalizations thereof. We are going to explore this aspect further in Sec. 6. For an infinite planar lattice the ground state of the Hamiltonian H^G is unique and can be explicitly computed. Note that there is a finite energy gap from the ground state to the excited states. Because the projection operators $A(v)$ and $B(p)$ are localized, excitations are particle-like living on vertices or plaquettes, or both, where the ground state condition (4.14) is violated. Classification of excitations, or quasiparticles, is a non-trivial problem. As a first step let us note some important properties of the operators $A^g(v)$ and $B^h(p,v)$. In the following we are going to call a combination of a plaquette p and a neighbouring vertex v a *site* and write $s = (p, v)$. Examples of sites are shown in Fig. 4.3.

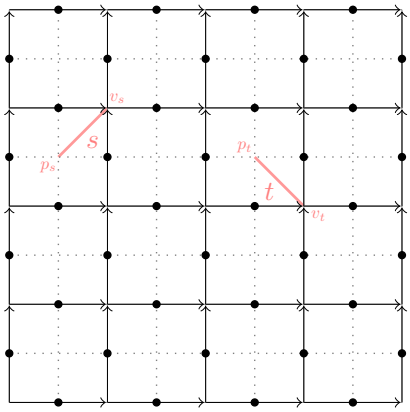

Figure 4.3: Examples of sites. The site s consists of the vertex v_s and the plaquette p_s, and t consists of the vertex v_t and the plaquette p_t. Throughout this work a given site $s = (p, v)$ will be represented by a line connecting v to the center of p.

For a given site $s = (p, v)$ the following relations hold for all $g, g', h, h' \in G$:

$$A^g(v)A^{g'}(v) = A^{gg'}(v), \tag{4.15}$$

$$B^h(s)B^{h'}(s) = \delta_{h,h'}B^h(s), \tag{4.16}$$

$$A^g(v)B^h(s) = B^{ghg^{-1}}(s)A^g(v). \tag{4.17}$$

The first equation shows that the mapping $g \mapsto A^g(v)$ defines a representation of G on $\otimes_e \mathbb{C}[G]$. Similarly, the mapping $P_h \mapsto B^h(s)$ defines a representation of $\mathcal{F}(G)$, where we have used the notation P_h from Sec. 3 to denote a basis element of $\mathcal{F}(G)$. The third equation reminds us of the multiplication rule for the elements of the Drinfeld double $D(G)$ that was introduced in Sec. 3, and in fact it turns out that the set of operators $\{B^h(s)A^g(v)|h, g \in G\}$ acting on the site $s = (p, v)$ generate an operator algebra $\mathcal{D}_s$ that is isomorphic to $D(G)$. For a detailed account on the Hopf-algebra axioms in this particular case see Ref. [1]. Note that the structure of this algebra does not depend on the particular site on which it acts. In the following sections we are going to refer to this algebra of operators as "the quantum double" and simply write $\mathcal{D}$ where it is not necessary to explicitly mention the corresponding site.

The excitations of the model are most conveniently classified in terms of so-called *elementary excitations*. These are excitations that violate the ground state condition (4.14) in a single site s. In Ref. [1] is is argued that this choice is justified, since any larger excitation can be shrunken down to the minimal size of a single site without affecting any other excitations that might be present. In the next subsection we define operators that create excitations at two sites s_0, s_1 of the lattice, and use these to classify the elementary particle types of the model.

4.2 Ribbon operators and particle types

From this point on, in order to avoid cluttering the notation, we are going to write A_v^g instead of $A^g(v)$ and B_s^h instead of $B^h(s)$. The goal of this subsection is to describe a set of operators which can create arbitrary particle-antiparticle

pairs from the ground state $|GS\rangle$ of the Hamiltonian H^G that was given in Eq. (4.13). Note that on a plane or on a sphere, charge conservation implies that a non-trivial excitation cannot exist on its own. However, on surfaces with non-trivial topology such single-particle states may be possible.

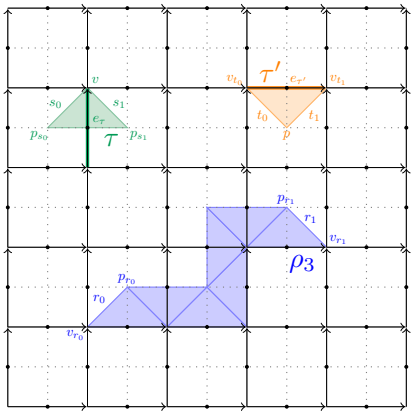

Figure 4.4: Examples of ribbons. ρ_1 is a dual triangle with endpoints s_0, s_1. ρ_2 is a dual triangle with endpoints t_0, t_1. ρ_3 is an arbitrary ribbon composed of 7 triangles and with endpoints given by r_0, r_1.

Consider the lattice shown in Fig. 4.4. Adjacent sites can be connected by triangles, where a triangle can belong to one of two types: Two adjacent sites $s_0 = (p_{s_0}, v)$, $s_1 = (p_{s_1}, v)$ that share the vertex v are connected by a triangle that is formed by s_0, s_1 and the dual edge connecting p_0 to p_1. Such a triangle is called a *dual triangle*. Two adjacent sites $t_0 = (p, v_{t_0})$, $t_1 = (p, v_{t_1})$ that share the plaquette p are connected by a triangle that is formed by t_0, t_1 and the direct edge connecting v_{t_0} to v_{t_1}. Such a triangle is called a *direct triangle*. Every triangle τ contains exactly one qudit situated at a direct edge e_τ of the lattice, see Fig. 4.4. Let us now define operators acting on this single qudit, depending on the type of triangle as well as the orientation of the edge e_τ:

$$L^h_{\tau_{dual}} = L^h(e_{\tau_{\text{dual}}}, v), \tag{4.18}$$

$$P^g_{\tau_{dir}} = P^g(e_{\tau_{\text{dir}}}, p), \tag{4.19}$$

for $h, g \in G$ and with the operators L^h and P^g defined according to Eqs. (4.7) and (4.8), respectively. Let us note that there is a certain choice regarding the definition of the starting site s_0 and the ending site s_1 of a triangle. In order to keep things simple, we will always label the starting and ending sites of a dual triangle such that (p_0, p_1, v) lists the corners of the triangle in counterclockwise order, and for a direct triangle we will label the starting and ending sites such that (v_0, v_1, p) lists the corners of the triangle in clockwise order. This convention can be reversed for a given triangle by reversing e_τ each time before the operators (4.18) or (4.19) are applied, and afterwards returning the edge to its original orientation.

In order to connect non-adjacent sites we can combine several triangles to form a *ribbon*. If the ending site s_1 of a triangle τ coincides with the starting

site t_0 of a second triangle τ', these triangles can be composed to form the ribbon $\rho = \tau\tau'$. In general, two ribbons are called *composable* if the ending site of the first ribbon coincides with the starting site of the second ribbon. We assume that the dual and the direct part of a ribbon each avoid self-crossing. An example of a ribbon consisting of multiple triangles is also shown in Fig. 4.4.

We now define operators acting on ribbons: For direct or dual triangles, respectively, we let

$$F^{h,g}_{\tau_{\text{dual}}} = \delta_{g,1} L^h_{\tau_{dual}}, \tag{4.20}$$

$$F^{h,g}_{\tau_{\text{dir}}} = P^g_{\tau_{dir}}, \tag{4.21}$$

where $L^h_{\tau_{dual}}$ and $P^g_{\tau_{dir}}$ were defined in Eqs. (4.18) and (4.19), respectively. The ribbon operators for longer ribbons are then defined recursively via the so-called *glueing relation*

$$F^{h,g}_{\rho} = \sum_{k\in G} F^{h,k}_{\rho_1} F^{k^{-1}hk,k^{-1}g}_{\rho_2}, \tag{4.22}$$

where $\rho = \rho_1\rho_2$ for two composable ribbons ρ_1, ρ_2. In the following we are going to assume that the starting site s_0 and the ending site s_1 of a ribbon ρ do not overlap. We call such ribbons *open* ribbons. The case of *closed* ribbons, for which we have $s_0 = s_1$, will be discussed later. The most important property of open ribbon operators is that an open ribbon operator $F^{h,g}_{\rho}$ commutes with all terms of the Hamiltonian H^G defined in Eq. (4.13) except for those corresponding to the starting site $s_0 = (p_0, v_0)$ and the ending site $s_1 = (p_1, v_1)$ of ρ. More explicitly, we have $[F^{h,g}_{\rho}, A_v] = [F^{h,g}_{\rho}, B_p] = 0 \quad \text{for } s_0, s_1 \neq s = (p, v)$ and

$$A^k_{v_0} F^{h,g}_{\rho} = F^{khk^{-1},kg}_{\rho} A^k_{v_0}, \tag{4.23}$$

$$B^k_{s_0} F^{h,g}_{\rho} = F^{h,g}_{\rho} B^{kh}_{s_0}, \tag{4.24}$$

$$A^k_{v_1} F^{h,g}_{\rho} = F^{h,gk^{-1}}_{\rho} A^k_{v_1}, \tag{4.25}$$

$$B^k_{s_1} F^{h,g}_{\rho} = F^{h,g}_{\rho} B^{g^{-1}h^{-1}gk}_{s_1}. \tag{4.26}$$

These relations can be obtained by a direct calculation using the glueing relation (4.22) as well as Eqs. (4.3)-(4.6). Moreover, the action of a ribbon operator $F^{h,g}_{\rho}$ does not explicitly depend on ρ, but only on its starting and ending sites s_0, s_1. That is, if ρ' is another ribbon with the same starting and ending sites, we have $F^{h,g}_{\rho}|GS\rangle = F^{h,g}_{\rho'}|GS\rangle$. Note that for a given ribbon ρ we have

$$F^{h,g}_{\rho} F^{h'g'}_{\rho} = \delta_{g,g'} F^{hh',g}_{\rho}, \tag{4.27}$$

$$(F^{h,g}_{\rho})^\dagger = F^{h^{-1},g}_{\rho}, \tag{4.28}$$

such that the n^2 ribbon operators for a given ribbon ρ connecting two sites s_0, s_1 generate an operator algebra $\mathcal{F}_\rho$ that is closed under Hermitian conjugation. It can be shown that all states with excitations only at s_0 and s_1 can be obtained by applying elements of $\mathcal{F}_\rho$ to the ground state $|GS\rangle$ [1]. Moreover, the generators $F^{h,g}_{\rho}$ can be shown to be linearly independent such that they form a basis of $\mathcal{F}_\rho$. From a more abstract point of view, it was argued in the original reference that the operator algebras $\mathcal{F}$ and $\mathcal{D}$ are dual to each other.

The space of two excitations at sites s_0 and s_1 is given by

$$\begin{aligned}\mathcal{L}(s_0, s_1) &= \{|\psi\rangle : A_v|\psi\rangle = B_s|\psi\rangle = |\psi\rangle \ \forall s = (p, v) \neq s_0, s_1\} \\ &= \text{span}\{F^{h,g}|GS\rangle | h, g \in G\}.\end{aligned} \tag{4.29}$$

Let us now consider the action of local operators acting on this space. In this context, an operator that acts locally on an excitation located at a site s is an operator that only acts on spins close to s in a way that it does not connect s to any other quasiparticle excitation. It can be shown that the algebra of local operators acting on a site s is simply given by the quantum double $\mathcal{D}_s$ [1]. For a pair of particles created from the ground state we obtain from Eqs. (4.23)-(4.26):

$$A^k_{v_0} F^{h,g}_\rho |GS\rangle = F^{khk^{-1},kg}_\rho |GS\rangle, \tag{4.30}$$

$$B^k_{s_0} F^{h,g}_\rho |GS\rangle = \delta_{k^{-1},h} F^{h,g}_\rho |GS\rangle, \tag{4.31}$$

where we have used the fact that $A^k_v|GS\rangle = |GS\rangle$ for all $k \in G$ and all vertices v of the lattice. The above action defines a representation of the quantum double $\mathcal{D}_{s_0}$ on $\mathcal{L}(s_0, s_1)$[2]. In fact, by sending the state $F^{h,g}_\rho|GS\rangle$ to $P_h g$ we can identify this action as the left multiplication of the quantum double and the corresponding representation as the regular representation. The regular representation can be decomposed into irreducible representations with the representation space $\mathcal{L}(s_0, s_1)$ splitting accordingly. We obtain

$$\mathcal{L}(s_0, s_1) = \bigoplus_\Pi n_\Pi V_\Pi, \tag{4.32}$$

where Π runs over all irreducible representations of $D(G)$, n_Π is used to denote the dimension of a given representation Π and $V_\Pi \subset \mathcal{L}(s_0, s_1)$ denotes the corresponding representation space. In other words, each irreducible representation of $\mathcal{D}_{s_0}$ corresponds to a subspace of the representation space $\mathcal{L}(s_0, s_1)$ that is invariant under the action of $\mathcal{D}_{s_0}$ given by Eqs. (4.30) and (4.31). These invariant subspaces can be interpreted as particle types since they correspond to localized conserved quantities. The particle types are therefore exactly given by the irreducible representations of the quantum double. Thus, the quantum double model has the same quasiparticle excitations as the anyon models that were presented in Sec. 3. In accordance with this theory, we interpret the vertex operators A^g_v as local gauge transformations and the plaquette operators B^h_s as the projectors onto the flux states $h \in G$. In this sense we say that the flux part of a particle at a given site $s = (p, v)$ is located at the plaquette p and is given by a violation of the corresponding plaquette stabilizer, whereas its charge part is located at the vertex v and is given by a violation of the corresponding vertex stabilizer. Each particle type can be thought of as carrying a particular internal Hilbert space given by V_Π. These additional degrees of freedom are a specific feature of Kitaev's quantum double models on a lattice and do not exist in the abstract anyon models emerging from discrete gauge theories. In order to avoid confusion we are going the refer to them as the *local* degrees of freedom of a given particle, whereas the internal degrees of freedom that we discussed in Sec. 3 will from now on be called the *topological* degrees of freedom. The parameters h and g of $F^{h,g}_\rho$ can now be interpreted in the following way. The local flux of the particle situated at the starting site s_0 is given by h or h^{-1}, depending on the orientation of the corresponding edge. g denotes the product of group elements or their inverses along a path on the direct lattice connecting s_0 to the ending site s_1. The flux of the particle at s_1 is then given by $g^{-1}hg$ or

[2] We could also use the site s_1 in this argument, which would give us the same quasiparticle types.

$g^{-1}h^{-1}g$. An explicit example of a ribbon operator acting on a ribbon consisting of 6 triangles is graphically represented in Fig. 4.5.

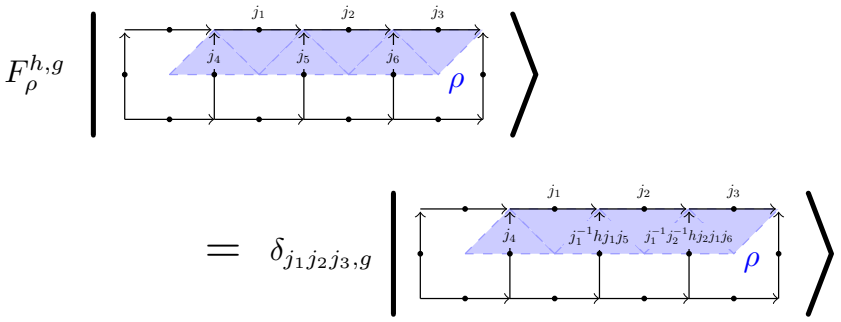

Figure 4.5: The action of a ribbon operator $F_\rho^{h,g}$ for a ribbon ρ composed of 6 triangles, as obtained by the glueing relation (4.22). The product of group elements along the direct part of the ribbon is projected onto g. If $F_\rho^{h,g}$ acts on the ground state of H^G, it creates a particle with local flux h^{-1} at s_0 and a particle with local flux $g^{-1}hg$ at s_1. We have chosen the orientation of the edges to match our standard orientation that is shown in Fig. 4.1.

As we have seen in Sec. 3, the irreducible representations of $D(G)$ are labelled by a conjugancy class $C \in (G)_{\text{conj}}$ and an irreducible representation $R \in (N_C)_{\text{irrep}}$. This makes it particularly easy to construct explicit projection operators onto the different particle types at a given site s. The projection onto the particles with flux $C \in (G)_{\text{conj}}$ is given by

$$P_s^{(\cdot,C)} = \sum_{c \in C} B_s^c. \tag{4.33}$$

Let us label the elements of C by $C = \{c_1, ..., c_{|C|}\}$. In order to further distinguish the particles, we are interested in irreducible representations of N_C, which we from now on fix as $N_C = N_{c_1}$. We denote a set of representatives for each equivalence class in G/N_C by $Q = \{q_1, ..., q_{|C|}\}$ such that $c_i = q_i c_1 q_i^{-1}$. We will always choose $q_1 = e$. For the pure charges, i.e. the particles with flux $C_1 = \{1\}$, a projector onto the subspace transforming under $R \in (G)_{\text{irrep}}$ can be constructed using the standard group-theoretical construction for the projector onto the subspace transforming under a given irreducible representation:

$$P_v^{(R,C_1)} = \frac{n_R}{|G|} \sum_{g \in G} \chi_R(g)^* A_v^g, \tag{4.34}$$

where χ_R is used to denote the character of the representation R. In the case of pure fluxes and dyons, the flux and charge part are interrelated as for a given flux $c_i \in C$ the charge part is given by an irreducible representation of the centralizer N_{c_i}. The projector onto the particle corresponding to (R, C) is then given by

$$P_s^{(R,C)} = \frac{n_R}{|N_C|} \sum_{i=1}^{|C|} B_s^{c_i} \sum_{n \in N_C} \chi(n)^* A_v^{q_i n q_i^{-1}}. \tag{4.35}$$

In order to immediately identify a ribbon operator with the type of the particle-antiparticle pair that it creates, it is useful to consider a different basis for the algebra of ribbon operators $\mathcal{F}$ [12]. For each $C \in (G)_{\text{conj}}$ and $R \in (N_C)_{\text{irrep}}$ define Q_C as before and label the elements of C and Q_C accordingly. For each irreducible representation $R \in (N_C)_{\text{irrep}}$ we choose a particular basis of the corresponding subspace and denote the representation matrices in this basis by $\Gamma_R(g)$ for $g \in N_C$. The dimension of R will be denoted by n_R. Then we write the new basis $F_\rho^{(R,C);\mathbf{uv}}$ as

$$F_\rho^{(R,C);\mathbf{uv}} = \frac{n_R}{|N_C|} \sum_{n \in N_C} \Gamma_R^{jj'}(n)^* F_\rho^{c_i^{-1}, q_i n q_{i'}^{-1}} \tag{4.36}$$

for $\mathbf{u} = (i, i')$, $\mathbf{v} = (j, j')$, where $i, i' \in \{1, ..., |C|\}$ and $j, j' \in \{1, ..., n_R\}$. A ribbon operator $F_\rho^{(R,C);\mathbf{uv}}$ creates a particle-antiparticle pair with topological charges (R, C), $(R^*, \bar{C})$ at sites s_0, s_1 when applied to the ground state $|GS\rangle$. This can be seen from the commutation relations (4.23)-(4.26) together with Eq. (4.35) for the projectors onto the elementary particle types.

The parameters $\mathbf{u}$ and $\mathbf{v}$ correspond to the local degrees of freedom of the particles located at both sides of the ribbon. More explicitly, i and j correspond to the local flux and charge degrees of freedom at s_0, whereas i' and j' correspond to the local flux and charge degrees of freedom at s_1. For $\mathbf{u} = (i, i')$, $\mathbf{v} = (j, j')$ it was shown in Ref. [12] that the following relations hold:

$$B_{s_0}^{c_k} B_{s_1}^{(c_{k'})^{-1}} F_\rho^{(R,C);\mathbf{uv}} |GS\rangle = \delta_{i,k} \delta_{i',k'} F_\rho^{(R,C);\mathbf{uv}} |GS\rangle, \tag{4.37}$$

$$A_{v_0}^{q_k^{-1} q_i} A_{v_1}^{(q_{k'})^{-1} q_{i'}} F_\rho^{(R,C);\mathbf{uv}} |GS\rangle = F_\rho^{(R,C);\tilde{\mathbf{u}}\mathbf{v}} |GS\rangle \tag{4.38}$$

with $\tilde{\mathbf{u}} = (k, k')$. Thus the local flux degrees of freedom can be changed by applying operations from the quantum double acting on the corresponding site. Furthermore, we have

$$a_{R'}^{kl} a'^{k'l'}_{\bar{R}'} F_\rho^{(R,C);\mathbf{uv}} |GS\rangle = \delta_{R,R'} \delta_{l,j} \delta_{l'j'} F_\rho^{(R,C);\mathbf{u}\tilde{\mathbf{v}}} |GS\rangle \tag{4.39}$$

with $\tilde{\mathbf{v}} = (k, k')$ and $a_{R'}^{kl} \in D_{s_0}$, $a'^{k'l'}_{R'} \in D_{s_1}$ defined by

$$a_R^{kl} = \frac{n_R}{|N_C|} \sum_{n \in N_C} \Gamma_R^{kl}(n)^* A_{v_0}^{q_i^{-1} n q_i}, \tag{4.40}$$

$$a'^{kl}_R = \frac{n_R}{|N_C|} \sum_{n \in N_C} \Gamma_R^{kl}(n)^* A_{v_1}^{q_{i'}^{-1} n q_{i'}}. \tag{4.41}$$

Therefore, the local charge degrees of freedom can also be measured and changed locally. Again let us emphasize that these degrees of freedom are a specific feature of Kitaev's quantum double models on a lattice and do not occur in the abstract anyon models emerging from discrete gauge theories.

For a two-particle state the only non-local degree of freedom is the type of the particles. For a multi-particle state the particle types and the local degrees of freedom carried by each particle can be found in a similar way as in the case of a two-particle state. However, there may be other non-local degrees of freedom associated with higher-dimensional fusion spaces of multiple non-Abelian anyons. It is shown in Ref. [1] that the space of n elementary excitations

of the types $d_1, ..., d_n$ located at the sites $s_1, ..., s_n$ can be described as

$$\mathcal{L}^{d_1,...d_n}_{s_1,...,s_n} = \mathcal{K}^{d_1}_{s_1} \otimes ... \otimes \mathcal{K}^{d_n}_{s_n} \otimes \mathcal{M}, \tag{4.42}$$

where the spaces $\mathcal{K}^{d_i}_{s_i}$ correspond to the space of local subtypes carried by a particle of the type d_i located at the site s_i. $\mathcal{M}$ is the topologically protected subspace corresponding to non-local degrees of freedom that are associated with the distinguishable fusion channels of the constituent particles. Unfortunately, this space does not have a tensor product structure, but its resilience against local perturbations makes it a good place to store quantum information. It is interesting to see how the topological degrees of freedom manifest in the explicit construction via ribbon operators, and how they can be manipulated in order to use them as a resource for topological quantum computation. This is going to be the main subject of Sec. 4.3.

First, however, let us briefly discuss the case of closed ribbon operators. Consider a ribbon σ whose starting and ending sites coincide, i.e. $s_0 = s_1 = s = (p, v)$. If σ consists of only dual triangles, it encloses exactly one vertex, whereas if it consists of only direct triangles, it encloses exactly one plaquette. We call such ribbons dual and direct closed ribbons, respectively. Both of these definitions are illustrated in Fig. 4.6. The vertex operators A^g_v and the plaquette operators B^h_s can be expressed by attaching suitable ribbon operators to these ribbons:

$$A^g_v = F^{g,1}_{\sigma_1}, \tag{4.43}$$

$$B^h_s = F^{1,h}_{\sigma_2}, \tag{4.44}$$

where σ_1 is a dual ribbon enclosing v and σ_2 is the direct ribbon with starting/ending site s that encloses p. Adapting the nomenclature from Ref. [12] we call a closed ribbon that consists of at least one dual and one direct triangle a *proper* closed ribbon. In the case of a proper closed ribbon that encloses exactly one site $s = (p, v)$, it is possible to express the quasiparticle occupancy projectors that were given in Eq. (4.35) as ribbon operators

$$P^{(R,C)}_s = \frac{n_R}{|N_C|} \sum_{i=1}^{|C|} \sum_{n \in N_C} \chi_R(n)^* F^{q_i n q_i^{-1}, q_i c_1 q_i^{-1}}_{\sigma} \tag{4.45}$$

with $\sigma = \sigma_1\sigma_2$, where again σ_1 is a dual ribbon enclosing v and σ_2 is the direct ribbon with starting/ending site s that encloses p. In fact the above projectors commute with *all* terms A_v, B_p of the Hamiltonian and thus "forget" their single end s. It is now natural to ask what set of operators commutes with all terms of the Hamiltonian if we consider arbitrary closed ribbons. The answer is given in Ref. [12]: For a proper closed ribbon σ the ribbon operators that commute with all vertex and plaquette operators form an algebra that is linearly generated by operators of the form

$$K^{(R,C)}_{\sigma} = \frac{n_R}{|N_C|} \sum_{i=1}^{|C|} \sum_{n \in N_C} \chi_R(n)^* F^{q_i n q_i^{-1}, q_i c_1 q_i^{-1}}_{\sigma}. \tag{4.46}$$

These have the exact same form as the operators defined in Eq. (4.45), with the only difference that σ now may enclose several sites instead of only one. In

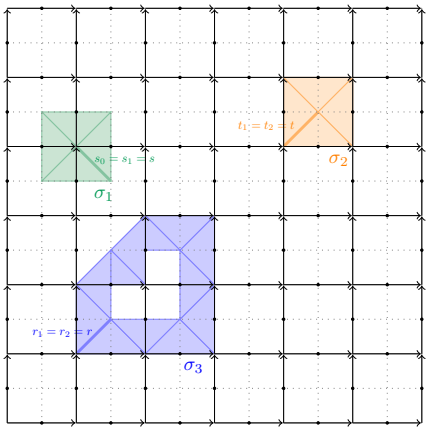

Figure 4.6: Exapmles of closed ribbons. σ_1 is a dual closed ribbon with starting/ending site s and encloses a single vertex. σ_2 is a direct closed ribbon with starting/ending site t and encloses a single plaquette. σ_3 is a proper closed ribbon, consisting of both dual and direct triangles.

fact it can be shown that the projectors $K_\sigma^{(R,C)}$ for a proper closed ribbon σ form a complete set of orthogonal projectors. For a given particle (R, C), the operator $K_\sigma^{(R,C)}$ projects onto the states with total charge (R, C) in the area that is enclosed by σ. Thus, the operators $K_\sigma^{(R,C)}$ can be used to measure the charge inside a given region of the lattice.

4.3 Braiding and fusion

This section contains only a very simplified outline of the constructions in the original paper [1]. The goal is to give an intuitive picture of the structure underlying the space $\mathcal{L}_{s_1,...,s_n}^{d_1,...,d_n}$ in terms of ribbon operators, while the technical arguments are completely omitted. However, this section should help readers who are new to the field to make the ideas presented in the original reference more accessible.

In order to establish a description of the topological degrees of freedom in a multi-particle system let us consider a useful picture that was introduced by Kitaev in his original paper [1]. Consider an n-particle state and suppose that the particles are connected to a common base site s_0 different from $s_1, ..., s_n$ by n non-intersecting ribbons $F_{\rho_1}, ..., F_{\rho_n}$, see Fig. 4.7. Since there is no excitation at s_0 the degrees of freedom that are associated with the end of each ribbon at the s_0 should, as a whole, transform trivially under the action of the quantum double D_{s_0}. However, for fixed internal states of the particles situated at $s_1, ..., s_n$, there may be multiple ways of how these particles can be connected to s_0 such that the vacuum constraint on s_0 is satisfied. This is a direct manifestation of the multiple distinguishable ways in which n non-Abelian anyons with vacuum total fusion channel can be fused back to the vacuum. As a simple (in fact, almost trivial) illustration of this idea let us consider a particle-antiparticle pair that was created from the vacuum. The glueing relation provides us with a means to "split" the ribbon ρ at an arbitrary site $s \neq s_0, s_1$ that lies within the ribbon ρ in order to obtain the decomposition $\rho = \rho_1\rho_2$, where ρ_1 has

the starting site s_0 and the ending site s and ρ_2 has the starting site s and the ending site s_1. The site s now has of course vacuum anyonic occupancy and is connected to both particles situated at s_0 and s_1, respectively. It thus corresponds to a possible choice of base site in the above construction. The topological degrees of freedom associated with each particle now correspond to the degrees of freedom located at the site s, or more specifically, the topological degree of freedom corresponding to the first particle corresponds to the degree of freedom of F_{ρ_1} located at its ending site s and the topological degree of freedom corresponding to the second particle corresponds to the degree of freedom of F_{ρ_2} located at its starting site s. In fact, by inspection of the particle-antiparticle creation operators together with the glueing relation (4.22) we gain the insight that for a pair of pure fluxes or charges created from the vacuum, the state of the topological degrees of freedom at s obtained in this way is exactly given by the states (3.16) or (3.17), respectively, that were discussed in the previous subsection. Similar results can be found for dyonic combinations and states consisting of more than two particles. Thus, in the Kitaev model the topological degrees of freedom of the abstract theory can be thought of as hiding "inside" the ribbon operators that connect several particles. However, let us emphasize that the explicit choice of s in the above example is unphysical.

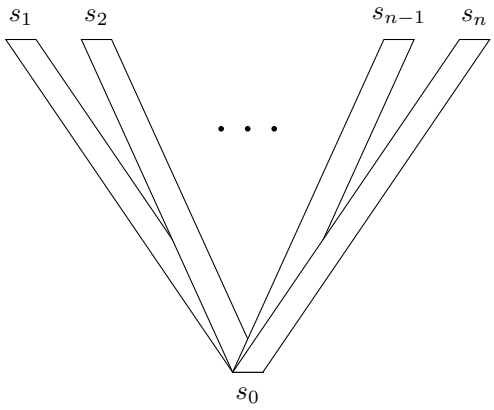

Figure 4.7: n particles situated at sites s_i, $i \in \{1, ..., n\}$ that are connected to the common base site s_0 by non-intersecting ribbon operators. The topological degrees of freedom correspond to the degrees of freedom corresponding to the site s_0 of each ribbon. The effect of braiding two particles can be calculated using the commutation relations between the corresponding ribbon operators, and the effect on the topological degrees of freedom coincides with the effect of the braiding operation that was introduced in Sec. 3.

The braiding operation of two neighbouring particles can now be computed by employing certain commutation relations between ribbon operators. It turns out that with this particular choice of connecting the ribbons to a common base site these commutation relations realize the exact braiding operations that were introduced for the abstract anyon models from Sec. 3 even for single exchanges. In general, only full monodromies will be realized in accordance with the general theory. Since the braiding operation corresponds to applying commutation relations that affect the ends of the ribbons located at the shared base site s_0, the internal degrees of the particles located at the sites s_1,...,s_n are not affected by braiding operations.

The effect of fusing two particles can be described by glueing the corresponding ribbons. In opposition to what might be intuitive, the local degrees of freedom do *not* affect the fusion outcome in any way, nor can they in general be used to predict the fusion outcome. This can be anticipated from the fact that it is possible to create particle-antiparticle pairs from the vacuum for *any* combination of internal degrees of freedom of the two particles, see Eq. (4.36).

In the next section we extend the quantum double models to a lattice with boundary. This introduces a variety of new phenomena such as quasiparticle condensation and confinements, and provides additional flexibility when designing schemes for topological quantum computation.

5 The quantum double model with boundary

In this section we generalize the quantum double models defined on an infinite planar lattice to the case with boundaries. Such a construction was first contemplated in Ref. [13] for the $D(\mathbb{Z}_2)$ quantum double model. Later similar constructions for arbitrary quantum double models were proposed in different variations, see for example Refs. [12, 14, 15]. In Sec. 5.1 we review an explicit Hamiltonian realization of the quantum double model with gapped boundaries, focusing on the aspects most relevant to topological quantum computation and referring the reader to the original references for more details. Sec. 5.2 generalizes this construction to the case of gapped domain walls between two topological phases, one associated with the quantum double model based on a finite group G and the other one associated with the quantum double model based on a possibly different finite group G'.

5.1 Gapped boundaries

In order to introduce gapped boundaries for the quantum double model, we modify the Hamiltonian H^G that was given in Eq. (4.13) following Ref. [12]. We first introduce the original construction but then make some slight adaptions in order to obtain the model that is best fit for our purposes. For two subgroups $N < M < G$ with N normal in G let us define the following operators acting on the single edge e_τ contained in a direct triangle τ_{dir} or in a dual triangle τ_{dual},

respectively:

$$L^N_{\tau_{\text{dual}}} = \frac{1}{|N|} \sum_{n \in N} L^n_{\tau_{dual}}, \tag{5.1}$$

$$T^M_{\tau_{\text{dir}}} = \sum_{m \in M} P^m_{\tau_{dir}}, \tag{5.2}$$

with $L^n_{\tau_{\text{dual}}}$, $P^m_{\tau_{\text{dir}}}$ defined according to Eqs. (4.18), (4.19). Since M is a subgroup of G, $T^M_{\tau_{\text{dir}}}$ does not depend on the orientation of the corresponding triangle τ_{dir}, and the normality constraint on N ensures the same for $L^N_{\tau_{\text{dual}}}$. As such, it is justified to label the operators by the single edge e that they act on instead of the triangle τ_{dual}, which is why we write L^N_e and T^M_e from now on. The fact that N is a subgroup of M ensures that the different terms commute, i.e. $[L^N_e, T^M_{e'}] = 0 \ \forall e, e'$. Furthermore, let us modify the plaquette stabilizers B^G_p and the vertex stabilizers A^G_v that were given in Eqs. (4.11) and (4.12), respectively, such that they commute with the single edge operators L^N_e, T^M_e by setting

$$A^M_v = \frac{1}{|M|} \sum_{m \in M} A^m_v, \tag{5.3}$$

$$B^N_p = \sum_{n \in N} B^n_s. \tag{5.4}$$

Note that $[A^M_v, B^N_p] = 0 \ \forall p, v$ since N is normal in G. For the same reason B^N_p does not depend on v. We now define the Hamiltonian

$$H^{M,N} = -\sum_v A^M_v - \sum_p B^N_p - \sum_e (L^N_e + T^M_e), \tag{5.5}$$

where the sums run over all vertices v, all plaquettes p and all edges e of the lattice, respectively. Like H^G the new Hamiltonian $H^{N,M}$ is also gapped and has localized excitations. These are combinations of vertex excitations, plaquette excitations and edge excitations. Classification of these excitations is a highly non-trivial problem and has been studied in Ref. [12] for some specific cases. In the sector without edge excitations, however, we actually deal with $|M/N|$-level spins instead of $|G|$-level spins. One can therefore intuitively anticipate that in this sector we now have an effective $D(M/N)$ quantum double model instead of the original $D(G)$ model, a fact which is formally proved in Ref. [12]. In this context the edge terms can be viewed as an explicit symmetry-breaking mechanism.

We can further generalize this construction by noting that in order for the terms of the Hamiltonian $H^{N,M}$ to commute, it is actually enough to have normality of N in M instead of normality of N in the full group G. The only complication is that in this case the edge terms L^N_τ, T^M_τ are no longer independent of the orientation of the lattice and we have to additionally choose an orientation of the boundary in order for the expressions (5.1) and (5.2) to be well-defined [16].

In the following discussion we focus on the case where $N = M$ and the topological order of the system is completely reduced to the vacuum. Obviously the looser normality constraint requiring that N is normal in M is automatically

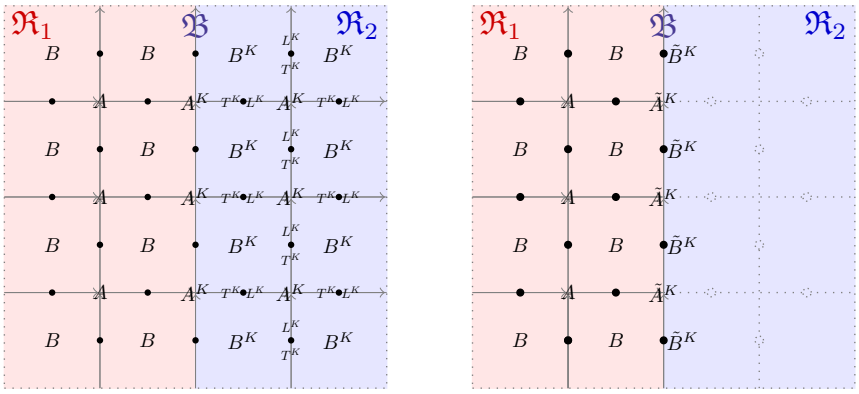

(a) (b)

Figure 5.1: (a) A gapped boundary between the $D(G)$ phase in $\mathfrak{R}_1$ and the vacuum in $\mathfrak{R}_2$ is engineered by a Hamiltonian acting on the vertices, plaquettes and edges of the lattice as indicated. For the definition of each term see the main text. (b) If we are interested in the sector without edge excitations, the qudits within the region $\mathfrak{R}_2$ can be removed from the code. This leads to 3-body vertex stabilizers $\tilde{A}^K$ and single qudit plaquette stabilizers $\tilde{B}^K$ along the boundary. These are also defined in the main text.

fulfilled in these cases. Let us write H^K instead of $H^{K,K}$ for the Hamiltonian defined in Eq. (5.5). The goal of this subsection is to consistently define a Hamiltonian that acts as H^G in a region $\mathfrak{R}_1$ and as H^K in a region $\mathfrak{R}_2$ of the lattice. We denote the dividing line between the two regions as the boundary $\mathfrak{B}$. For simplicity we choose the boundary to lie on the direct lattice; however, it would also be possible to consider boundaries that lie on the dual lattice, or boundaries that lie partly on the dual and partly on the direct lattice. Note that the terms A_v^G, B_s^G of the Hamiltonian H^G commute with the terms A_v^K, B_p^K of the Hamiltonian H^K. Therefore we can define the total Hamiltonian as follows: Let H^K act on all the vertices, plaquettes and edges within $\mathfrak{R}_2$, as well as on all the edges on the boundary $\mathfrak{B}$. On all the vertices, plaquettes and edges within $\mathfrak{R}_1$, as well as on all the edges on $\mathfrak{B}$ we impose the Hamiltonian H^G. This situation is visualized in Fig. 5.1(a). We can then write the total Hamiltonian as

$$H = H^G(\mathfrak{R}_1) + H^K(\mathfrak{R}_2), \tag{5.6}$$

where we fix the convention that we interpret all vertices and plaquettes on $\mathfrak{B}$ as belonging to $\mathfrak{R}_2$ and all edges on $\mathfrak{B}$ as belonging to $\mathfrak{R}_1$ for notational simplicity. It is now interesting to consider processes where a pair of quasiparticles is created in $\mathfrak{R}_1$ and then one quasiparticle is moved past the boundary into $\mathfrak{R}_2$. The extended ribbon operator now possibly creates i) a combination of a violated plaquette and vertex term of H^K at its ending site, and ii) a chain of edge excitations along the dual part of the ribbon that lies within $\mathfrak{R}_2$. Note that ii) is a specific feature of the symmetry-reduced Hamiltonian. We say that a vertex or plaquette excitation in $\mathfrak{R}_2$ for which ii) occurs is *confined*, as moving it requires an energy input that is proportional to the length of the corresponding ribbon. As a special case it is possible that neither i) or ii) occur. In this case the quasiparticle 'disappears' when it is moved past the boundary, i.e it

condenses to the vacuum in $\mathfrak{R}_2$. It can be shown that for $N = M = K$ i) and ii) only occur together, which means that every quasiparticle that does not get condensed to the vacuum is actually confined. In the following, we are going to focus on the particles that condense to the vacuum at the boundary.

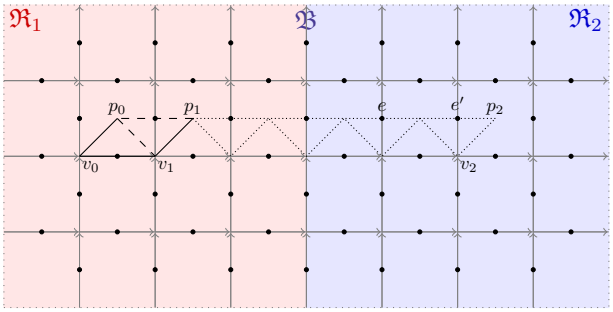

Figure 5.2: A pair of particles is created in the $D(G)$ phase at the sites $s_0 = (p_0, v_0)$ and $s_1 = (p_1, v_1)$ by a suitable ribbon operator. If this ribbon operator is extended past the boundary and up to the site $s_2 = (p_2, v_2)$, we get an excitation of H^K that possibly consists of a plaquette excitation at p_2, a vertex excitation at v_2 and edge excitations at the edges e, e'. The latter confine non-trivial excitations.

Note that if we are only interested in condensation to the vacuum, or equivalently in the sector without edge excitations, it is possible to redefine the lattice that is shown in Fig. 5.1(a) by removing the data qudits within $\mathfrak{R}_2$ from the code, as the edge projectors completely fix their state. The vertex and plaquette stabilizers along the boundary are now modified; the definition of the modified vertex stabilizers $\tilde{A}_v^K$ is the same as in Eq. (5.3) but acting on 3 qudits instead of four, since star(v) now only consists of 3 qudits. Similarly the modified plaquette stabilizers $\tilde{B}_p^K$ are defined as in Eq. (5.4) but act on a single qudit, since ∂p only consists of a single qudit. The edge terms of the Hamiltonian H^K are now redundant. From this point of view it is natural to say that the Hamiltonian H^G acts within the region $\mathfrak{R}_1$ and the Hamiltonian $\tilde{H}^K = -\sum_p \tilde{B}_p^K - \sum_v \tilde{A}_v^K$ acts on the boundary $\mathfrak{B}$, as the redefined plaquettes can now be attributed to the boundary. This situation is visualized in Fig. 5.1(b). We write

$$\tilde{H} = H^G(\mathfrak{R}_1) + \tilde{H}^K(\mathfrak{B}), \tag{5.7}$$

which coincides with the construction given by Beigi *et al.* in Ref. [14]. However, their construction allows for more flexibility as it additionally includes the possibility to modify the boundary based on a subgroup K by a 2-cocycle $\varphi \in H(K, \mathbb{C}^\times)$. The boundaries that we consider in this work are the ones corresponding to trivial 2-cocycles.

In order to systematically analyse condensation processes, we need to calculate the probability for a given anyon from the $D(G)$ phase to get condensed to the vacuum at the boundary. This can be done following the arguments of Ref. [12]. Let $|\psi_K\rangle$ be a ground state of H^K, i.e. a state that satisfies

$$A_v^K|\psi_K\rangle = B_s^K|\psi_K\rangle = L_e^K|\psi_K\rangle = T_e^K|\psi_K\rangle = |\psi_K\rangle \tag{5.8}$$

for all sites s and all vertices v within and on the boundary of $\mathfrak{R}_2$ as well as for all the edges e within $\mathfrak{R}_2$. Then we can calculate the expectation value of a closed

ribbon operator $K_\sigma^{(R,C)}$ corresponding to the projection onto a quasiparticle (R,C) with $C \in (G)_{\text{conj}}$ and $R \in (N_C)_{\text{irrep}}$, see Eq. (4.45):

$$\langle K_\sigma^{(R,C)} \rangle = \langle \psi_K | K_\sigma^{(R,C)} | \psi_K \rangle. \tag{5.9}$$

If this expectation value is non-zero, we have a non-zero probability to find the particle (R,C) in the ground state of the Hamiltonian H^K, i.e. it is possible for the particle (R,C) to get condensed to the vacuum at the boundary. According to Ref. [12] the expectation value is given by

$$\langle K_\sigma^{(R,C)} \rangle = \frac{n_R}{|N_C||K|} \sum_{i=1}^{|C|} \sum_{n \in N_C} \chi_R^*(n) \delta_{q_i c_1 q_i^{-1} \in K} \delta_{q_i n q_i^{-1} \in K}, \tag{5.10}$$

where the relevant notations were defined in Sec. 4.2. For K normal in G this can be simplified to

$$\langle K_\sigma^{(R,C)} \rangle = \frac{n_R}{|N_C||K|} |C \cap K| \langle \chi_R, 1 \rangle_{N_C \cap K}, \tag{5.11}$$

where 1 is used to denote the trivial representation of $N_C \cap K$ and $\langle \cdot, \cdot \rangle$ is the product of characters defined by

$$\langle \chi_R, \chi_{R'} \rangle_G = \frac{1}{|G|} \sum_{g \in G} \chi_R(g)\ \chi_{R'}(g)^*. \tag{5.12}$$

Expression (5.11) is non-zero if and only if i) $N \cap C \neq \emptyset$ and ii) the subduced representation of R onto $N_C \cap K$ contains the trivial representation of $N_C \cap K$ in its decomposition into irreducible representations. Note that if K is not normal in G the condensation behaviour of a particle (R,C) can depend on the local state of the particle as well, and a non-zero expectation value in Eq. (5.10) only tells us that there exists some local state of the particles that gets condensed to the vacuum. In most cases that are relevant to topological quantum computation, however, this information will be enough since we are only interested in the total topological charge located in the region $\mathfrak{R}_2$.[3] In particular, it can be seen from the above expression for $\langle K_\sigma^{(R,C)} \rangle$ that for an arbitrary group G the trivial subgroup $\{1\}$ always corresponds to the boundary where all the pure charges are condensed to the vacuum, whereas the subgroup G corresponds to the boundary where the pure fluxes are condensed.

Gapped boundaries can be used to store quantum information. More interestingly, they provide us with a way to perform topological quantum computation that does not require the existence of non-Abelian anyons. To see this, consider a pair of so-called *holes* h_1, h_2, which simply correspond to regions of the lattice where the original Hamiltonian has been replaced by a Hamiltonian H^{K_1}, H^{K_2} for $K_1, K_2 < G$ with the boundaries defined as above. The

[3] While Eqs. (5.10) and (5.11) only describe condensation to the vacuum, a complete algebraic description of the particle spectrum that can be obtained from condensing bulk anyons to the boundary can be found in Ref. [15]. From Theorem 2.12 in this reference a condensation rule similar to Eq. (5.11) can be obtained for arbitrary $K < G$; however, it did not become clear to me how this result is consistent with the above theory in the case of non-normal K. In particular, in the calculation of the condensation products for a bulk particle (R,C) there seems to be a dependency on the choice of representative r_C that I do not know how to resolve.

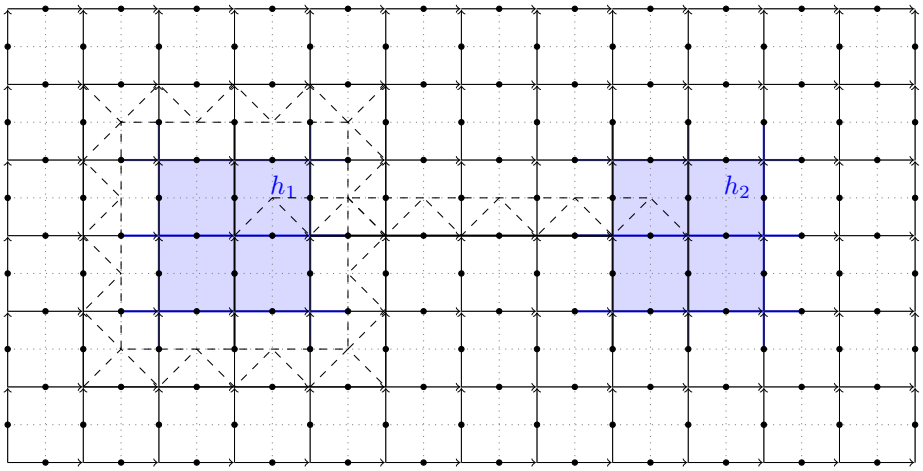

Figure 5.3: Two holes in the lattice. The Hamiltonian H^K acts on all the vertices on the boundary of the holes as well as on all plaquettes, vertices and edges within the holes. There is an additional ground state degeneracy associated with the different particle-antiparticle pairs that get condensed to the vacuum at the corresponding boundaries. Logical states can be associated with these different condensation channels. The corresponding space is topologically protected as long as the holes are large and well separated since the operators that act non-trivially on the condensation channels either have to connect both holes or completely encircle a single hole. Examples are indicated by dashed ribbons.

corresponding situation is shown in Fig. 5.3. It is now possible that a non-trivial ribbon operator creates a particle in h and its antiparticle in h' such that both particles get condensed to the vacuum at the corresponding boundaries. Then there is an additional ground state degeneracy associated with each particle-antiparticle pair that gets condensed in this way. We call these pairs the different *condensation channels* of the pair of holes. Provided the holes are large and well separated, the different condensation channels of the pair span a topologically protected space that can be used to store quantum information. In particular, d distinguishable condensation channels of a pair of holes can be associated with the d computational basis states of a qudit. Throughout this work, we will refer to this encoding as the *hole-pair encoding*. For the state corresponding to an anyon x that has condensed to the vacuum at h_1 and an anyon y that has condensed to the vacuum at h_2 we write $|xy\rangle$. As such, the condensation channels can also be interpreted as the net anyonic occupancy of the hole in terms of the anyons that get condensed. A logical operator acting on the topologically protected space while commuting with all stabilizer terms has to either have support on a ribbon connecting both holes or encircling one of the holes completely. Examples of such ribbons are also indicated in Fig. 5.3. Multiple pairs of holes can be introduced to encode multiple qudits. The information that is stored in this way can then be processed by braiding the holes or by performing certain non-topological operations like fusion. While in principle the movement of holes can be realized by adiabatically tuning the corresponding Hamiltonian, this is likely to be impractical in an actual experimental realization. Therefore holes are often used in a different implementation

of the quantum double models, where the actual Hamiltonian is replaced by repeated measurements of the quasiparticle occupancy of all the plaquettes and vertices. We are going to discuss this implementation in Sec. 6, after having generalized the construction of boundaries to arbitrary domain walls between two phases corresponding to different quantum double models.

5.2 Gapped domain walls

Consider a lattice that is divided into two half-planes $\mathfrak{R}_1$, $\mathfrak{R}_2$ as shown in Fig. 5.4(a). We associate the left half-plane with the quantum double model for a finite group G, and the right half-plane with the quantum double model for a possibly different finite group G'. As such there are $|G|$-level spins taking values in $\mathbb{C}[G]$ placed on each edge of the left half-plane and $|G'|$-level spins taking values in $\mathbb{C}[G']$ placed on each edge of the right half-plane. Along the line $\mathfrak{D}$ that divides the two parts we choose to have both types of spins sitting on each edge. Note that we choose this line to lie on the direct lattice, although a similar construction featuring a domain wall lying on the dual lattice would also be possible. The total Hamiltonian of the system should act as H^G in the left and $H^{G'}$ in the right half-plane. The question is now how to consistently define the terms of the Hamiltonian acting on the line that divides the two half-planes. This can be answered by employing the *folding idea* [14]. Imagine the lattice is folded along the line that divides the two half-planes, where we choose the convention that the right half-plane is folded over the left half-plane which stays in place. This leaves us with a half-plane that consists of two 'layers', one associated with the $D(G)$ phase and the other one with the $D(G')$ phase. In total we now have a $|G|$-level spin and a $|G'|$-level spin associated with each edge of the folded lattice which take values in $\mathbb{C}[G] \times \mathbb{C}[G'] \sim \mathbb{C}[G \times G']$. This situation is visualized in Fig. 5.4(c). We can now let the Hamiltonian $H^{G\times G'}$ act on the bulk of the folded plane, which effectively acts as H^G in the bulk of the layer corresponding to $D(G)$ and as $H^{G'}$ in the bulk of the layer corresponding to $D(G')$. The corresponding excitations are the excitations of the $D(G \times G')$ quantum double model, which are given by pairs consisting of an excitation of the $D(G)$ phase and an excitation of the $D(G')$ phase each. Note, however, that by folding the plane we have changed the orientation of the right half-plane. This means that in the layer corresponding to the right half-plane, clockwise and counterclockwise braidings are exchanged with respect to the unfolded plane. Mathematically this corresponds to sending the flux part of an anyon to its inverse, which is why a pair of anyons $\big((R, C), (R', C')\big)$ in the folded plane actually corresponds to a pair (R, C), $(R, \bar{C}')$ in terms of the unfolded plane. Again we have used $\bar{C}$ to denote the inverse conjugancy class of C. The terms acting along the domain wall can now easily be obtained by engineering a boundary for the $D(G \times G')$ quantum double model and then "unfolding" the plane. According to the last subsection the boundaries of the $D(G \times G')$ model can be parametrized by a subgroup $K < G \times G'$ (and a 2-cocycle $\varphi \in H^2(K, \mathbb{C}^\times)$ in the most general case). In the following we are going to use the simplified version of the boundary construction where no qudits are placed in the vacuum part of the code, see Sec. 5.1. The corresponding Hamiltonian for the folded plane is given by Eq. (5.5) and is visualized in Fig. 5.4(d) for completeness. The total Hamiltonian for the unfolded plane - though mathematically equivalent to

the one for the folded plane - can be written as

$$H = H^G(\mathfrak{R}_1) + H^{G'}(\mathfrak{R}_2) + \tilde{H}^K(\mathfrak{D}), \tag{5.13}$$

for clarity, with the different terms acting on the corresponding parts of the lattice as indicated in Fig. 5.4(b). Let us furthermore introduce the following intuitive notation for the domain wall stabilizers: For a vertex v that lies on the domain wall let v_l denote the left half of the vertex v, i.e. the three $|G|$-level spins that are adjacent to v, and let v_r denote the right half of the vertex v, i.e. the three $|G'|$-level spins that are adjacent to v. We can now write $\tilde{A}_v^K$ explicitly as

$$\tilde{A}_v^K = \sum_{(g,g')\in K} A_{v_l}^g \otimes A_{v_r}^{g'}. \tag{5.14}$$

Similarly, for a domain wall plaquette p let p_l denote the single associated $|G|$-level spin and let p_r denote the single associated $|G'|$-level spin. For a subgroup K that is a product of two subgroups $K_1 < G$, $K_2 < G'$ the vertex stabilizers $\tilde{A}_v^K$ acting on the domain wall can be written as a tensor product of operators acting on v_l and v_r, respectively. The same is true for the single qudit plaquette stabilizers $\tilde{B}_p^K$ in terms of p_l and p_r. In this case the domain wall can simply be interpreted as consisting of two boundaries, one for the $D(G)$ phase and one for the $D(G')$ phase, placed next to each other.

Note that the method described above gives us a domain wall which is static, i.e. it is fixed in its position and cannot be moved as the qudits on either side of the dividing line take values in different Hilbert spaces. However, the theory could be adapted by placing spins taking values in $\mathbb{C}[G \times G']$ at every edge of the (unfolded) lattice and projecting them onto $\mathbb{C}[G]$ for the left half-plane or $\mathbb{C}[G']$ for the right half-plane by suitable edge terms as discussed in Sec. 5.1. Note that yet another boundary between a $D(G)$ and a $D(H)$ quantum double model where $H < G$ can be constructed by employing the symmetry reduction mechanism that was presented in Sec. 5.1 with two different subgroups $N < M < G$ with N normal in G in order to break the symmetry in the right half-plane down to a subgroup $H = M/N < G$ as argued in Ref. [12]. However, in the sector without edge excitations this construction gives boundaries which are equivalent to certain boundaries obtained by the folding idea for suitable subgroups.

In order to investigate the tunneling of particles let us go back to the folded plane for an instant. Imagine a particle from the $D(G \times G')$ phase - which is effectively a pair of two particles, one from the $D(G)$ phase and the other from the $D(G')$ phase - is moving towards the boundary and condenses to the vacuum at the boundary. In the unfolded plane this corresponds to the process where a particle from the $D(G)$ phase and a particle from the $D(G')$ phase annihilate at the domain wall that divides the two phases, or, by reverting the movement of the second particle, to a process where the first particle crosses the domain wall without leaving behind a domain wall excitation and appears as the antiparticle of the second particle in the $D(G')$ phase. Recall that a pair of anyons $\big((R,C),(R',C')\big)$ in the folded plane corresponds to a pair (R,C), $(R',\bar{C}')$ in terms of the unfolded plane. Thus, condensing an anyon pair $\big((R,C),(R',C')\big)$ to the vacuum at the boundary of the folded plane actually corresponds to a tunneling of (R,C) to (R'^*,C') in the unfolded plane. In Sec. 9 we construct a domain wall between a $D(\mathbb{Z}_2)$ quantum double model and a $D(S_3)$ quantum

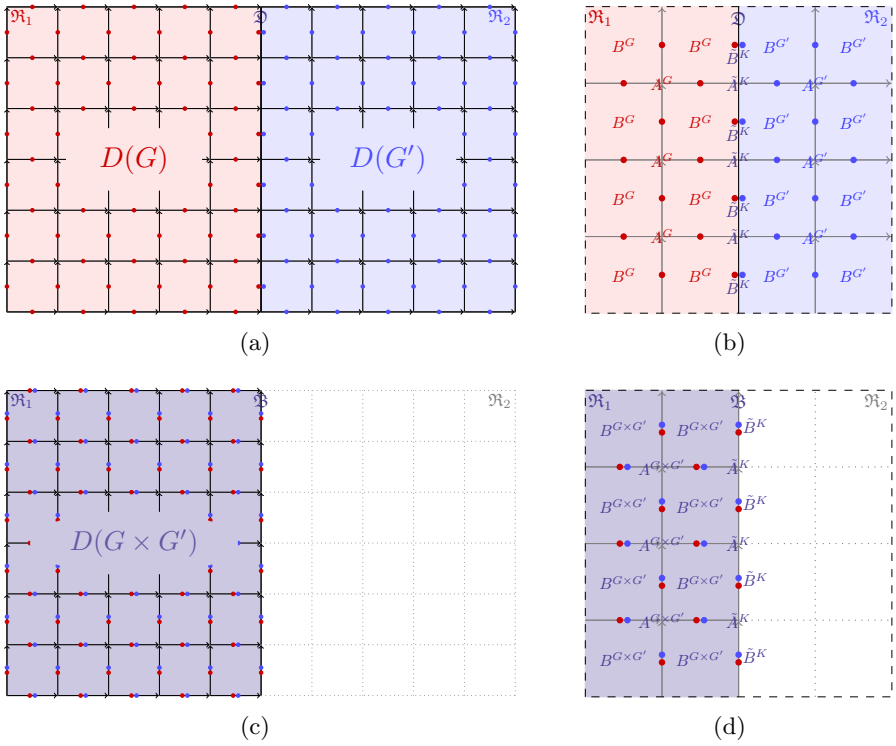

Figure 5.4: (a) The lattice is divided into two half-planes, with the left half-plane associated with the $D(G)$ quantum double model for a finite group G and the right half-plane associated with the $D(G')$ quantum double model for a possibly different finite group G'. $|G|$-level spins indicated as red dots are placed on each edge of the $D(G)$ part of the lattice, and $|G'|$-level spins indicated as blue dots are placed on each edge of the $D(G')$ part of the lattice. Along the line that divides the two half-planes we have both a $|G|$-level and a $|G'|$-level spin. (b) Terms of the Hamiltonian acting near the domain wall separating the $D(G)$ phase from the ($D(G')$ phase. The corresponding notations were introduced in the main text of this section as well as in Sec. 5.1. (c) By folding the plane along the line that divides the two half-planes, the situation shown in a) becomes equivalent to a single half-plane corresponding to the $D(G \times G')$ quantum double model with a boundary to the vacuum. In the $D(G \times G')$ part of the lattice we have a $|G|$-level and a $|G'|$-level spin placed on each edge. (d) Terms of the Hamiltonian acting near the boundary of the $D(G \times G')$ phase. The corresponding notations were introduced in Sec. 5.1.

double model, resulting in what we call a *hybrid quantum double model*. We use this construction to not only move quasiparticles from one phase to the other but also the information carried by the quasiparticle occupancy of certain holes. We investigate under which circumstances such a process is possible while keeping the information protected at all times and give a detailed protocol how this can be achieved in a specific case. First, however, we give a short summary of how arbitrary quantum double models can be realized using generalized stabilizer circuits.

6 Generalized stabilizer circuits

Engineering a Hamiltonian of the form (4.13), (5.5) or (5.13) with actual 4-body interactions is rather involved in practice. In order to physically realize Kitaev's $D(\mathbb{Z}_2)$ quantum double model Dennis and Kitaev proposed an implementation that simulates the Hamiltonian $H^{\mathbb{Z}_2}$ using local stabilizer circuits, see Ref. [17]. This was further investigated by Fowler et al. in Refs. [18, 19]. A brief outline of how these techniques can be generalized to arbitrary $D(G)$ quantum double models was recently given by Cong *et al.* in Ref. [15]. Here we follow their approach, additionally commenting upon some details concerning non-Abelian quantum double models.

When implementing quantum double models as stabilizer codes we repeatedly perform measurements in order to keep track of the anyonic occupancy of all the vertices and plaquettes. Interaction with the environment causes errors on the qudits comprising the code, which manifest themselves as unwanted quasiparticle excitations. Decoding algorithms can then be applied in order to determine the most probable way in which these excitations were created such that they can be fused accordingly. This removes the unwanted excitations, preventing them from interacting with the logical information encoded in the system. Finding suitable error correction procedures for non-Abelian quantum double models is a highly non-trivial problem which we are not going to tackle in this work. A review of error correction in general and in the $D(\mathbb{Z}_2)$ surface codes as a particular example can be found in Ref. [20]. Error detection and correction procedures for non-Abelian models were considered in Refs. [21, 22].

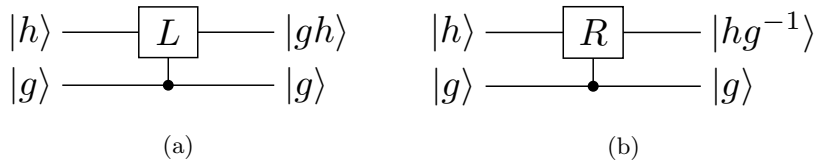

Figure 6.1: Definition of controlled multiplications for qudits taking values in the group algebra $\mathbb{C}[G]$ for a finite group G. (a) Definition of the controlled left multiplication. (b) Definition of the controlled right multiplication.

Let us consider an arbitrary finite group G and the corresponding quantum double model. Let $s = (p, v)$ be a site. According to the definition of the plaquette operators B_s^h, see Eq. (4.10), the flux around p is calculated by taking the ordered product of group elements (or their inverses) corresponding to the states of the spins in ∂p. If the flux around p is h, the charge residing at the vertex v is given by the irreducible representation according to which the four qudits in $\mathrm{star}(v)$ transform under local gauge transformations A_v^g for $g \in N_h$. This is most easily captured in the form of the explicit projection operators onto the different quasiparticle types at s that were given in Eq. (4.35). In order to realize suitable stabilizer circuits, let us introduce controlled left and right multiplication gates for arbitrary group elements $g \in G$ as shown in Fig. 6.1. These gates can be considered generalizations of the well-known CNOT gate, which can be recovered from the definition in Fig. 6.1 in the case of $G = \mathbb{Z}_2 = \{1, x\}$ for $g = x$. Let us place an additional ancillary qudit at each plaquette and each vertex. These are needed to measure the flux and

charge on the corresponding plaquettes and vertices, respectively. In order to distinguish between the ancillary qudits and the actual qudits comprising the code we call the former the *syndrome qudits* and the latter the *data qudits*. We now proceed to construct circuits that simulate the Hamiltonian H^G. In a first step we focus on Abelian quantum double models. Since for Abelian groups each element forms its own conjugancy class, the fluxes of the model are simply labelled by elements of G. The centralizer of every group element is equal to the whole group. As such all charges correspond to irreducible representations of G itself. Furthermore, for Abelian groups all the irreducible representations are one-dimensional. Therefore all the irreducible representations of the quantum double $D(G)$ are one-dimensional as well and the local subspaces carried by the particles are trivial. In other words, there are no local degrees of freedom in the case of Abelian models. In particular, note that the fluxes and charges are not interrelated in this case and all the projection operators that were given in Eq. (4.35) can be written as tensor products of an operator measuring the flux at the plaquette p and an operator measuring the charge at vertex v. To perform the flux measurement for a given plaquette p we use the plaquette syndrome qudit in order to accumulate the ordered product of group elements (or their inverses) corresponding to the states of the spins in ∂p. Measurement of the plaquette syndrome qudit in the basis $\{|h\rangle | h \in G\}$ then projects the flux onto a certain flux state $|h\rangle$. The corresponding circuit is shown in Fig. 6.2(a). For the charge measurement on a vertex v we first prepare the vertex syndrome qudit in the state $|1\rangle$[4] and apply an inverse Fourier transform corresponding to the group G on this qudit. We then perform controlled left or right multiplications with the syndrome qudit as the control and the data qudits located at the edges in $\mathrm{star}(v)$ as the target, depending on their orientation with respect to v. Application of a Fourier transform and subsequent measurement of the vertex syndrome qudit then projects out a charge state transforming according to a particular irreducible representation R of G. The corresponding circuit is shown in Fig. 6.2(c). These measurement circuits are now performed simultaneously for all the plaquettes and vertices of the lattice. They are periodically repeated in order to give reliable information about the quasiparticle occupancy at each vertex and each plaquette. If the flux around a plaquette p is consistently measured to be $h \in G$, then an anyon with flux h resides on the corresponding plaquette. If the vertex v is consistently measured to transform under the irreducible representation R of G, then an anyon with charge R lives on the corresponding vertex.

In the case of non-Abelian quantum double models the extraction of the syndrome information can be a bit more involved. In general the projectors B_s^h do not commute with all the vertex operators A_v^g, see Eq. (4.17), and the particle types are given by projectors that cannot necessarily be written as a tensor product of a charge and a flux part. Complete extraction of the syndrome information would thus not be possible via simultaneous flux and charge measurements. However, applying the true quasiparticle projectors would introduce a severe time overhead in the error correction framework. If we accept certain

[4]In order to keep our notation consistent with the previous sections, we use $|1\rangle$ to denote the ground state of the qubits that comprise the $D(\mathbb{Z}_2)$ surface codes. This is in contrast to the standard (additive) notation, where the ground state of a qubit is denoted by $|0\rangle$. For the logical qubits introduced later in this work, however, we will fall back on this more conventional notation.

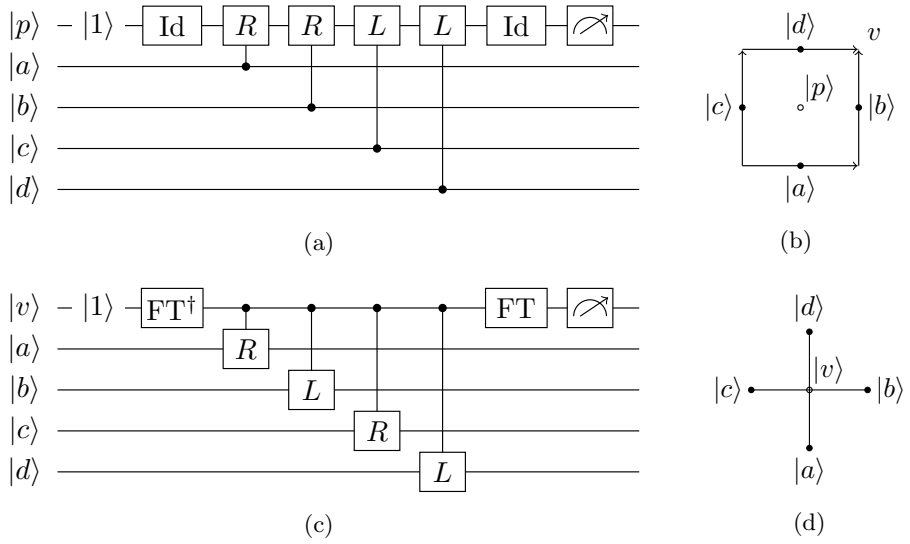

Figure 6.2: (a) Stabilizer circuit that measures the flux around a plaquette p, starting and ending at the top right neighbouring vertex v. The plaquette syndrome qudit is denoted as p by a slight abuse of notation, and the data qudits in ∂p are labelled a to d. (b) The convention for labelling the data qudits around the plaquette p. The zig-zag sequence is crucial in order for neighbouring circuits not to interfere with each other. (c) Stabilizer circuit that measures the irreducible representations of G according to which the qudits in star(v) transform under local gauge transformations A_v^g. The vertex syndrome qudit is denoted as v and the data qudits in star(v) are labelled a to d. (d) The convention for labelling the data qudit around v. Again particular attention must be paid to the specific ordering of the labels.

limitations concerning the syndrome information that can be obtained, it is still possible to use simultaneous vertex and plaquette measurements. For the theory of Fourier transforms corresponding to general (non-Abelian) groups and their explicit implementation see Ref. [23]. Note that the definition of the plaquette circuit shown in Fig. 6.2(a) implicitly fixes a choice of sites for the particles to reside on; by choosing to evaluate all fluxes with respect to the starting and ending vertex v at the top right corner of p, the syndrome information is given in terms of the anyonic occupancy of sites of this form. As in the Abelian case all circuits operate in lockstep. Let $s = (p, v)$ denote a particular site of the form specified above. If the order of the controlled operations on the qubits in star(v) and ∂p is chosen as indicated in Figs. 6.2(d) and Fig. 6.2(b), respectively, the circuit for v touches the shared qudits before the circuit for p does. The vertex circuits were designed in a way that they measure the irreducible representation of G according to which the qudits in star(v) transform under local gauge transformations A_v^g for $g \in G$. However, for a flux in the conjugancy class C we need to know according to which irreducible representation of N_C the corresponding qudits transform under local gauge transformations of N_C. Since the restriction of an irreducible representation of G onto N_C is not necessarily irreducible, it will in general not be possible to distinguish all the dyons in the particle spectrum of the model. However, depending the structure of G and its subgroups, it may still be possible to reliably detect certain dyonic types. An

example will be discussed later in the context of the non-Abelian $D(S_3)$ model. Additionally, operators containing off-diagonal elements of higher-dimensional representations may cause rotations in the local charge subspace carried by a given particle. After the vertex circuit the plaquette circuit touches the shared qudits. The fact that this circuit does not commute with the vertex cicuit is now reflected in the following way. The flux eigenstate $|h\rangle$ resulting from the measurement of the plaquette syndrome qudit does indeed correspond to the actual flux of the particle *after* the full stabilizer circuit cycle. However, this state does not necessarily reflect the original flux state *before* this measurement round, since the vertex circuit at v may have mixed the local flux states of the particle within the conjugancy class C_h. Still, the flux measurement gives us the correct conjugancy class of the particle located at (p, v) and the correct local flux state after the vertex measurement. Moreover, the local flux state before the vertex measurement can in principle be inferred from the outcome of this measurement and the structure of the irreducible representations of G. Since we do not use the local degrees of freedom for quantum computational purposes, the rotations that appear as a side-effect of the stabilizer circuits do not cause any problems from a theoretical point of view.

Let us now consider the implementation of suitable stabilizer circuits for the boundary Hamiltonians H^K. In general, the implementation of these circuits strongly depends on the properties of the physical system that is used in order to experimentally realize the spin lattice model and should be discussed individually in each case. Nevertheless, let us make a few general comments. In order to realize the boundary Hamiltonian (5.5) we need to implement the single spin stabilizers L_e^N and T_e^M given in Eqs. (5.1) and (5.2), respectively. For $N = M = K$ the simultaneous eigenspace of these two operators acting on an edge e is one-dimensional. Therefore it is in principle possible to complete this single simultaneous eigenstate to a basis of $\mathbb{C}[G]$ and then perform single spin measurements in this basis on all edges of the lattice, provided that the physical system allows such a measurement. Alternatively, one could also imagine using an additional edge syndrome qudit and a suitable stabilizer circuit if the data qudits themselves are not addressable. In order to realize the vertex stabilizers A_v^K or $\tilde{A}_v^K$, respectively, we may place an additional vertex syndrome qudit at each vertex and then apply a stabilizer circuit corresponding to the subgroup K instead of the whole group G. The implementation of the plaquette stabilizers B_p^K or $\tilde{B}_p^K$ again depends on the measurements that are possible in a particular physical system. In this work we are going to use the charge holes corresponding to the trivial subgroup $K = \{1\}$ in order to store and process information. These are particularly simple to implement, as the stabilizer circuits for the single edge terms amount to single-spin measurements in the basis $\{|g\rangle | g \in G\}$. The vertex stabilizer circuits inside and on the boundaries of the holes are now turned off completely, whereas the plaquette stabilizer circuits operate in the same way as before.

The stabilizer formalism also gives us a convenient means to create, move and annihilate holes adapting the techniques that were discussed in Ref. [18,19]. Holes are created by turning off the stabilizer circuits corresponding to H^G in a certain region of the lattice and instead turning on the stabilizer circuit corresponding to the Hamiltonian H^K in this area. In the case of charge holes this can be achieved by single spin measurements as described above. Outcomes that do not correspond to the state $|1\rangle$ should be corrected or accounted for

in the (classical) control software in order to maintain error detection. Holes are moved by subsequent expansion and contraction processes, i.e. by turning on the stabilizer circuits for H^K in a region that we want to include in the hole and reinforcing the stabilizer circuits for H^G in a region that should no longer be part of the hole. In order to enlarge a charge hole, a region of spins along the boundary is measured in the basis $\{|g\rangle|g \in G\}$, again correcting for inappropriate measurement outcomes. Then the hole is contracted by reinforcing the vertex stabilizers in the area that should no longer be part of the hole. The measurement outcomes on these vertices are now random and outcomes corresponding to non-trivial quasiparticles should be moved into the hole in order to preserve the total quasiparticle occupancy of the hole. Note that when moving holes in the presence of a Hamiltonian this Hamiltonian has to be adapted according to each step of the movement, as else the superpositions of different quasiparticles that may be present inside the hole would be prone to decohere. Since this demands a lot of flexibility from the experimental control of the system, codes that use holes in order to process quantum information are often implemented as pure stabilizer codes, i.e. without the presence of a corresponding Hamiltonian. Details on the fault-tolerance of processes involving the manipulation of holes can be found in the original references in the case of the $D(\mathbb{Z}_2)$ code, which can be adapted to other quantum double models as well. However, we will not discuss this in detail here.

7 The $D(\mathbb{Z}_2)$ quantum double model

In this section we focus on the group $\mathbb{Z}_2 = \{1, x\}$ where 1 denotes the identity element and x is an element with $x^2 = 1$. $\mathbb{Z}_2$ is the simplest non-trivial group; it is Abelian and furthermore cyclic. This allows significant simplifications to the general theory that was presented in the previous sections. In Sec. 7.1 we apply the theory that was presented in Sec. 3 in order to determine the particle spectrum of the $D(\mathbb{Z}_2)$ anyon model, and in Sec. 7.2 we review the quantum double model based on the group $\mathbb{Z}_2$ as introduced in Sec. 4. In Sec. 7.3 we briefly summarize the standard computational schemes that are currently used in order to perform topological quantum computation in the $D(\mathbb{Z}_2)$ model.

7.1 Particle spectrum

As for any Abelian group, every element of $\mathbb{Z}_2$ is its own conjugancy class and all irreducible representations of $\mathbb{Z}_2$ are one-dimensional. Explicitly, we have the two conjugancy classes $C_1 = \{1\}$ and $C_x = \{x\}$. The two inequivalent irreducible representations of $\mathbb{Z}_2$ are the trivial representation $\rho_1^{[+]}$ and the signed representation $\rho_1^{[-]}$ given by

$$\rho_1^{[+]}(1) = 1, \qquad \rho_1^{[+]}(x) = 1, \tag{7.1}$$

$$\rho_1^{[-]}(1) = 1, \qquad \rho_1^{[-]}(x) = -1. \tag{7.2}$$

Note that we chose the subscript 1 in order to indicate the dimension of the representation, as in the following chapters we are going to deal with groups that additionally have higher-dimensional irreducible representations. Thus there are four particles in the $D(\mathbb{Z}_2)$ spectrum. These are summarized in Table 7.1. The

Particle	1	e	m	ϵ
Conjugancy class C	C_1	C_1	C_x	C_x
Irreducible representation of N_C	$\rho_1^{[+]}$	$\rho_1^{[-]}$	$\rho_1^{[+]}$	$\rho_1^{[-]}$

Table 7.1: The particle spectrum of the $D(\mathbb{Z}_2)$ model. For the definition of the notations see the main text.

particle given by the trivial conjugancy class together with the trivial representation corresponds to the anyonic vacuum, i.e. the absence of any quasiparticle. For the non-trivial particles we use the historical nomenclature: The pure flux corresponding to the conjugancy class C_x and the trivial representation is called m as in *magnetic*, whereas the pure charge corresponding to the trivial conjugancy class and the signed representation is called e as in *electric*. The dyon corresponding to the conjugancy class C_x and the signed representation is most commonly denoted by ϵ.

The fusion rules for this anyon model are listed in Table 7.2. In particular, each particle is its own antiparticle and the ϵ particle is the composite of an e and an m particle. Since there are no higher-dimensional fusion spaces, all the F-matrices are trivial. The non-trivial full monodromies are

$$\begin{aligned} R^2_{em} = R^2_{me} = -1, \qquad & R^2_{e,\epsilon} = R^2_{\epsilon,e} = -1, \\ R^2_{m,\epsilon} = R^2_{\epsilon,m} = -1, \qquad & R_{\epsilon,\epsilon} = -1. \end{aligned} \tag{7.3}$$

Note that even though the e and m quasiparticles behave as bosons with respect to themselves, they exhibit anyonic mutual exchange statistics. The ϵ particle has fermionic self-statistics.

$\times$	1	e	m	ϵ
1	1	e	m	ϵ
e	e	1	ϵ	m
m	m	ϵ	1	e
ϵ	ϵ	m	e	1

Table 7.2: The fusion rules for the $D(\mathbb{Z}_2)$ anyon model.

7.2 Spin-lattice realization

In order to realize the $D(\mathbb{Z}_2)$ anyon model on a lattice we place a qubit at each edge and introduce suitable vertex and plaquette operators as defined in Sec. 4.1. Note that in this case it is not necessary to define an orientation of the edges since $\mathbb{Z}_2$ is Abelian and each element of $\mathbb{Z}_2$ is its own inverse. In fact we find

$$L^1_+ = L^1_- = \mathrm{Id}, \qquad L^x_+ = L^x_- = \sigma^x, \tag{7.4}$$

$$P^1_+ = P^1_- = |1\rangle\langle 1|, \qquad P^x_+ = P^x_- = |x\rangle\langle x|, \tag{7.5}$$

where σ^x denotes the Pauli-X operation. The plaquette and vertex stabilizers explicitly read

$$A_v = \frac{1}{2}(\mathbb{1} + \prod_{j \in \mathrm{star}(v)} \sigma_j^x), \tag{7.6}$$

$$B_p = \frac{1}{2}(\mathbb{1} + \prod_{j \in \partial p} \sigma_j^z), \tag{7.7}$$

which can be obtained from Eqs. (4.11) and (4.12) by a straightforward calculation. Again, $\mathrm{star}(v)$ is used to denote the four spins adjacent to the vertex v, and ∂p denotes the boundary of the plaquette p. Furthermore, σ_j^x and σ_j^z denote the Pauli-X and Pauli-Z matrices acting on the qubit j, respectively. The Hamiltonian is defined according to Eq. (4.13),

$$H^{\mathbb{Z}_2} = -\sum_v A_v - \sum_p B_p, \tag{7.8}$$

where the sums run over all the vertices v and all the plaquettes p of the lattice, respectively. Actually, $H^{\mathbb{Z}_2}$ can be cast into an even simpler form since up to rescaling and a constant shift it is equivalent to

$$H^{\mathbb{Z}_2} = -\sum_v \prod_{j \in \mathrm{star}(v)} \sigma_j^x - \sum_p \prod_{j \in \partial p} \sigma_j^z, \tag{7.9}$$

which is the form that is most commonly found in literature. Note that since the terms of the Hamiltonian are elements of the Pauli group, the $D(\mathbb{Z}_2)$ quantum double model is an example of a stabilizer code in its original definition as given in Refs. [11, 24]. The implementation of the $D(\mathbb{Z}_2)$ quantum double model using stabilizer circuits can be obtained from Sec. 6 in a straightforward way and has been extensively studied in the corresponding literature (see for example Refs. [18, 19]), which is why we are not going to give further details here.

In the case of Abelian models the ribbon operators from Sec. 4.2 simplify significantly. In fact, for the $D(\mathbb{Z}_2)$ quantum double model the ribbon operators for the e and m anyons are simply given by strings of σ^x or σ^z operations acting along a sequence of spins forming a path on the dual or direct lattice, respectively. Examples of such string operators are shown in Fig. 7.1. The ϵ particles can be moved by a combined application of an e and an m string operator. This is also indicated in Fig. 7.1 . Note that from the commutation relations between σ_j^x and σ_j^z it can immediately be verified that the commutation relations between the e and m string operators reproduce the correct braiding rules (7.3) for full monodromies of the $D(\mathbb{Z}_2)$ quasiparticles.

To conclude this summary of the $D(\mathbb{Z}_2)$ quantum double model let us consider the gapped boundaries of the model. There are two types of gapped boundaries for the $D(\mathbb{Z}_2)$ quantum double model, corresponding to the two trivial subgroups $K_1 = \{1\}$ and $K_2 = \mathbb{Z}_2$. The particles that condense to the vacuum at each boundary can easily be determined by Eq. (5.11) or by direct inspection of the plaquette and vertex stabilizers in H^K. In the case of $K = K_1$ the anyons which are condensed to the vacuum are the pure charges 1 and e, whereas for $K = K_2$ the pure fluxes 1 and m are condensed to the vacuum. In the following sections, we adapt the convention that we label each boundary by

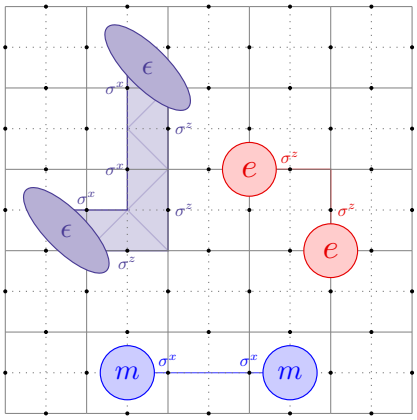

Figure 7.1: Examples of ribbon operators that can create and move quasiparticles in the $D(\mathbb{Z}_2)$ quantum double model. Note that since the charge parts and the flux parts of the particles are not interrelated, the ribbon operators simplify to strings of Pauli operators acting on paths of spins on the dual or direct lattice. This is why these operators are usually referred to as *string operators*.

the anyons that get condensed at this boundary. In the case of the $D(\mathbb{Z}_2)$ quantum double model we are thus going to distinguish between $1+e$ boundaries and $1+m$ boundaries, and similarly between $1+e$ holes and $1+m$ holes. Note that in the literature on the $D(\mathbb{Z}_2)$ surface codes the $1+e$ boundaries (holes) are often referred to as rough boundaries (holes), and the $1+m$ boundaries (holes) are called smooth boundaries (holes).

7.3 Computational power

In the context of topological quantum computation the $D(\mathbb{Z}_2)$ model on a planar lattice is most commonly referred to as the $D(\mathbb{Z}_2)$ *planar* or *surface code*. There are multiple ways of encoding a logical qubit in the surface codes. If suitable boundary terms are introduced a single logical qubit can be stored in the corresponding edge occupancy, see Refs. [13, 17]. However, with this approach only one qubit can be stored per code. In order to perform operations between several qubits, several codes need to be interacted either transversally or via so-called lattice surgery [25]. The standard way to store and manipulate several logical qubits in a single $D(\mathbb{Z}_2)$ surface code is the introduction of holes as described in Sec. 5.1. Logical qubits are then stored in the condensation channels of pairs of either $1+e$ or $1+m$ holes. Another way to encode qubits in the surface codes is the engineering of so-called *defects*, which can be shown to exhibit the same projective braid statistics as Majorana zero modes. A unifying description of these different encodings as well as procedures to switch between them can be found in Ref. [26]. In general, the operations that can be performed fault-tolerantly in the $D(\mathbb{Z}_2)$ surface codes are the operations belonging to the *Clifford group* $\mathcal{C}_n$. Let us briefly recall the relevant definitions. The Pauli group $\mathcal{P}_n$ on n qubits is defined as

$$\mathcal{P}_n = \{\pm 1, \pm i\} \times \{\mathbb{1}, \sigma^x, \sigma^y, \sigma^z\}^{\otimes n}, \tag{7.10}$$

where the operators σ^a for $a \in \{x, y, z\}$ are used to denote the usual single qubit Pauli-X, Pauli-Y and Pauli-Z operators, respectively. The Clifford group $\mathcal{C}_n$ is defined as the normalizer of the Pauli group in the group $\mathcal{U}_n$ of unitary transformations on n qubits,

$$\mathcal{C}_n = \{U \in \mathcal{U}_n \mid UPU^{-1} \in \mathcal{P} \ \ \forall P \in \mathcal{P}\}. \tag{7.11}$$

States that can be prepared by Clifford operations alone are called *stabilizer states*. Non-stabilizer states are going to play an important role in the following sections. While the Clifford operations on their own are not sufficient to perform universal quantum computation, the additional injection of ancillary non-stabilizer states can be used to construct a universal gate set. In the following sections, in particular in Sec. 9, we assume that we are able to fault-tolerantly perform arbitrary Clifford operations in the $D(\mathbb{Z}_2)$ surface codes. We focus on the case where logical qubits are encoded in the anyonic occupancy of pairs of $1 + e$ holes. However, we are not going to expand on how the particular Clifford operations are realized in this encoding as these techniques have extensively been discussed in the corresponding literature. Note that in principle it is also possible to employ the techniques presented in Ref. [26] to temporarily switch from the $1 + e$ hole-pair encoding to another one if desired.

8 The $D(S_3)$ quantum double model

After having reviewed the $D(\mathbb{Z}_2)$ planar code as the simplest of the quantum double models, we are now moving on to the slightly more complicated case of $D(S_3)$. The symmetric group S_3 is the smallest non-Abelian group, which makes this a particularly suitable example to study some of the specific features of non-Abelian quantum double models. In Sec. 8.1 we describe the particle spectrum of the $D(S_3)$ anyon model following the abstract theory that was presented in Sec. 3, and in Sec. 8.2 we study the corresponding spin lattice realization. In Sec. 8.3 we give a short summary of the current approaches to performing topological quantum computation with the $D(S_3)$ quantum double model.

8.1 Particle spectrum

S_3 is the group of permutations of a set of three elements, which we are going to label $\{1, 2, 3\}$ for convenience. It consists of 6 elements; these are the identity 1, the three transpositions (1 2), (2 3) and (1 3), and the two 3-cycles (2 3 1) and (2 1 3). S_3 is generated by the two elements $x = (1\ 2)$ and $y = (2\ 1\ 3)$ and we can write

$$S_3 = \{1, x, y, yx, y^2, y^2x\}, \tag{8.1}$$

Note that x and y satisfy the relations

$$xy = y^2x, \ x^2 = 1, \ y^3 = 1. \tag{8.2}$$

Thus, from a more abstract point of view, S_3 is the group generated by two letters x and y modulo the relations (8.2), i.e.

$$S_3 = < x, y \mid xy = y^2x, x^2 = 1, y^3 = 1 > . \tag{8.3}$$

g	Centralizer N_g of g	Isomorphy class of N_g
1	$\{1, x, y, yx, y^2, y^2x\}$	S_3
x	$\{1, x\}$	$\mathbb{Z}_2$
y	$\{1, y, y^2\}$	$\mathbb{Z}_3$
yx	$\{1, yx\}$	$\mathbb{Z}_2$
y^2	$\{1, y, y^2\}$	$\mathbb{Z}_3$
y^2x	$\{1, y^2x\}$	$\mathbb{Z}_2$

Table 8.1: The centralizer N_g of each element $g \in S_3$. Note that the centralizers for elements of the same conjugancy class are isomorphic.

There are three distinct conjugancy classes of S_3, which are given by $C_1 = \{1\}$, $C_x = C_{yx} = C_{y^2x} = \{x, yx, y^2x\}$ and $C_y = C_{y^2} = \{y, y^2\}$, as can easily be verified by direct calculation. According to Sec. 3 these label the flux types of the $D(S_3)$ anyon model. In the following we choose to represent these three conjugancy classes by the fiducial elements 1, x and y and write C_1, C_x and C_y, respectively. In order to determine the particle types of the model we calculate the centralizer for all the elements $g \in S_3$. The result can be found in Table 8.1. For the pure charges, i.e. the particles with flux C_1, we are interested in the irreducible representations of S_3. There are 3 inequivalent irreducible representations of S_3, namely the trivial representation $R_1^{[+]}$, the signed representation $R_1^{[-]}$ and the two-dimensional representation R_2. They are given by

$$R_1^{[+]}(g) = 1 \quad \forall g \in S_3, \tag{8.4}$$

$$R_1^{[-]}(g) = \begin{cases} 1 \text{ for } g \in \{1, y, y^2\} \\ -1 \text{ for } g \in \{x, yx, y^2x\} \end{cases}, \tag{8.5}$$

$$\begin{aligned} R_2(1) &= \begin{pmatrix} 1 & 0 \\ 0 & 1 \end{pmatrix}, \qquad R_2(x) = \begin{pmatrix} 0 & 1 \\ 1 & 0 \end{pmatrix}, \qquad R_2(y) = \begin{pmatrix} \omega & 0 \\ 0 & \bar{\omega} \end{pmatrix}, \\ R_2(yx) &= \begin{pmatrix} 0 & \omega \\ \bar{\omega} & 0 \end{pmatrix}, \qquad R_2(y^2) = \begin{pmatrix} \bar{\omega} & 0 \\ 0 & \omega \end{pmatrix}, \qquad R_2(y^2x) = \begin{pmatrix} 0 & \bar{\omega} \\ \omega & 0 \end{pmatrix} \end{aligned} \tag{8.6}$$

with $\omega = e^{\frac{2\pi i}{3}}$. For the particles with flux C_x the charge part is given by a unitary irreducible representation of $\mathbb{Z}_2$. The two inequivalent irreducible representations of $\mathbb{Z}_2$ were already given in Eqs. (7.1) and (7.2) in Sec. 7. Similarly, for the particles with flux C_y one finds the inequivalent irreducible representations of $\mathbb{Z}_3$ to be $\rho_1^{[1]}$, $\rho_1^{[\omega]}$, $\rho_1^{[\bar{\omega}]}$ given by

$$\rho_1^{[1]}(1) = 1, \qquad \rho_1^{[1]}(y) = 1, \qquad \rho_1^{[1]}(y^2) = 1, \tag{8.7}$$

$$\rho_1^{[\omega]}(1) = 1, \qquad \rho_1^{[\omega]}(y) = \omega, \qquad \rho_1^{[\omega]}(y^2) = \bar{\omega}, \tag{8.8}$$

$$\rho_1^{[\bar{\omega}]}(1) = 1, \qquad \rho_1^{[\bar{\omega}]}(y) = \bar{\omega}, \qquad \rho_1^{[\bar{\omega}]}(y^2) = \omega, \tag{8.9}$$

again with $\omega = e^{\frac{2\pi i}{3}}$. Thus, the particle spectrum of the $D(S_3)$ anyon model consists of 8 particles which we are going to label A through H. They are listed in Table 8.2.

Particle	A	B	C	D	E	F	G	H
Conjugancy class C	C_1	C_1	C_1	C_x	C_x	C_y	C_y	C_y
Irreducible representation of N_C	$R_1^{[+]}$	$R_1^{[-]}$	R_2	$\rho_1^{[+]}$	$\rho_1^{[-]}$	$\rho_1^{[1]}$	$\rho_1^{[\omega]}$	$\rho_1^{[\bar{\omega}]}$

Table 8.2: The particle spectrum of $D(S_3)$. There are 8 particles, denoted A through H, corresponding to the 8 distinct pairs of a conjugancy class $C \in (G)_{\text{conj}}$ and an irreducible representation $R \in (N_C)_{\text{irrep}}$.

Once the particle types are determined, one can find the fusion rules of the $D(S_3)$ quantum double model by applying Eqs. (3.9) and (3.10). The result is summarized in Table 8.3. Note that there are several subsystems which are closed under fusion. To be specific, these are the subsystems

$$\{A,B\},\quad \{A,B,C\},\quad \{A,B,F\},\quad \{A,B,G\},\quad \{A,B,H\},$$
$$\{A,B,F,G\},\quad \{A,B,F,H\},\quad \{A,B,G,H\},\quad \{A,B,F,G,H\}.$$

We do not give a complete list of the F and R matrices of the model because of its immense length, and instead refer the reader to the appendix of Ref. [27]. In Sec. 9, however, we explicitly introduce a particular braiding matrix that will be used to perform a quantum gate.

$\times$	A	B	C	D	E	F	G	H
A	A	B	C	D	E	F	G	H
B	B	A	C	E	D	F	G	H
C	C	C	$A+B+C$	$D+E$	$D+E$	$G+H$	$F+H$	$F+G$
D	D	E	$D+E$	$A+C$ $+F+G+H$	$B+C$ $+F+G+H$	$D+E$	$D+E$	$D+E$
E	E	D	$D+E$	$B+C$ $+F+G+H$	$A+C$ $+F+G+H$	$D+E$	$D+E$	$D+E$
F	F	F	$G+H$	$D+E$	$D+E$	$A+B+F$	$C+H$	$C+G$
G	G	G	$F+H$	$D+E$	$D+E$	$C+H$	$A+B+G$	$C+F$
H	H	H	$F+G$	$D+E$	$D+E$	$C+G$	$C+F$	$A+B+H$

Table 8.3: The fusion rules for the $D(S_3)$ anyon model.

8.2 Spin-lattice realization

In order to realize the $D(S_3)$ model on a lattice following Kitaev's quantum double model construction, we need to place 6-level spins that take values in S_3 on each edge of the lattice. A system that naturally provides such a structure might be hard to find. However, an important fact that may simplify the experimental realization of the $D(S_3)$ quantum double model is that S_3 is the semi-direct product of $\mathbb{Z}_3$ and $\mathbb{Z}_2$,

$$S_3 = \mathbb{Z}_3 \rtimes \mathbb{Z}_2. \tag{8.10}$$

As such it is possible to use a qubit and a qutrit in order to build up a 6-level system which takes values in S_3. More explicitly, recall that the definition of the semi-direct product is as follows. For a group G let $\text{Aut}(G)$ denote the group of automorphisms of G. Then, for two groups H, K and a homomorphism

$\phi : K \to \mathrm{Aut}(H)$, $k \mapsto \phi_k$, we can define a group structure on the set of elements $\{(h,k) \,|\, h \in H,\, k \in K\}$ by defining the multiplication

$$(h,k)(h',k') = (h\phi_k(h'), kk'). \tag{8.11}$$

The identity element is then given by $(1,1)$ and the inverse of an element (h,k) by $(h,k)^{-1} = (\phi_k^{-1}(h^{-1}), k^{-1})$. On the other hand, suppose that we have two subgroups H, K of a group G such that the following conditions hold: i) H is normal in G, ii) $H \cap K = \{1\}$ and iii) $HK = G$. Let ϕ be the homomorphism $\phi : K \to \mathrm{Aut}(H)$, $k \mapsto \phi_k$ with $\phi_k(h) = khk^{-1}$ for $h \in H$. Then G is isomorphic to the semi-direct product $H \rtimes K$ and an element $g \in G$ is identified with a pair (h,k) with $h \in H$ and $k \in K$. In the case of S_3 we have $S_3 \sim \mathbb{Z}_3 \rtimes \mathbb{Z}_2$. As seen previously, every element $g \in S_3$ can be written in the form $g = y^r x^s$ with $r \in \{0,1,2\}$ and $s \in \{0,1\}$. The left and right multiplication operators acting on the composite 6-level system in terms of the qubit-qutrit basis $|r\rangle|s\rangle = |y^r x^s\rangle$ are then given by

$$\begin{aligned}
L_+^1 &= \mathrm{Id}_3 \otimes \mathrm{Id}_2, & L_-^1 &= \mathrm{Id}_3 \otimes \mathrm{Id}_2,\\
L_+^x &= \mathrm{swap}(1,2) \otimes \sigma_x, & L_-^x &= \mathrm{Id}_3 \otimes \sigma_x,\\
L_+^y &= X \otimes \mathrm{Id}_2, & L_-^y &= X \otimes |0\rangle\langle 0| + X^{-1} \otimes |1\rangle\langle 1|,\\
L_+^{yx} &= \mathrm{swap}(0,1) \otimes \sigma_x, & L_-^{yx} &= X^{-1} \otimes |0\rangle\langle 1| + X \otimes |1\rangle\langle 0|,\\
L_+^{y^2} &= X^{-1} \otimes \mathrm{Id}_2, & L_-^{y^2} &= X^{-1} \otimes |0\rangle\langle 0| + X \otimes |1\rangle\langle 1|,\\
L_+^{y^2x} &= \mathrm{swap}(0,2) \otimes \sigma_x, & L_-^{y^2x} &= X \otimes |0\rangle\langle 1| + X^{-1} \otimes |1\rangle\langle 0|.
\end{aligned} \tag{8.12}$$

Here, Id_d is used to denote the identity operation on a d-level system, X_3 denotes the generalized Pauli-X on a qutrit and $\mathrm{swap}(i,j)$ denotes the operation that swaps the i-th and the j-th basis state of the qutrit. The left and right multiplication operators $L_\pm^g$ can now be used to construct the vertex projectors A_v. The single qudit projection operators $P_\pm^h$ in the qubit-qutrit basis are simply given by the tensor product of the projections onto the corresponding states of the qubit and the qutrit. These can be used to construct the plaquette projectors B_p. The A_v and the B_p terms can then be used to engineer the Hamiltonian H^G. Alternatively, the left and right multiplication operators as well as the projection operators can be used to build up suitable stabilizer circuits as described in Sec. 6. It turns out that all the particles of the $D(S_3)$ particle spectrum with flux C_1 or C_y can be distinguished by simultaneous plaquette and vertex measurements as defined in Fig. 6.2, given that we are willing to accept certain rotations in the local subspaces of the corresponding particles. In fact, the operations resulting from the vertex measurement circuit defined in Fig. 6.2(c) correspond to projections onto irreducible representations of $\mathbb{Z}_3$ as well, combined with a rotation in the local charge subspace in the case of the one-dimensional representations as well as the off-diagonal elements of R_2. The particles D and E corresponding to the conjugancy class C_x cannot always be distinguished by the syndrome information that is obtained in this way.

In order to gain some general intuition for the model it is useful to explicitly write down the projectors onto the different particle types. These can easily be found from the particle spectrum of $D(S_3)$ and the projection operators that were given in Eq. (4.35). Let $s = (p,v)$ be a site. Then we get the following

projectors onto the pure charges located at s:

$$P_v^A = \frac{1}{6}\big(A_v^1 + A_v^x + A_v^y + A_v^{yx} + A_v^{y^2} + A_v^{y^2x}\big), \tag{8.13}$$

$$P_v^B = \frac{1}{6}\big(A_v^1 - A_v^x + A_v^y - A_v^{yx} + A_v^{y^2} - A_v^{y^2x}\big), \tag{8.14}$$

$$P_v^C = \frac{1}{3}\big(2A_v^1 - A_v^y - A_v^{y^2}\big). \tag{8.15}$$

If the flux around p is given by the conjugancy class C_x, we find the projections onto the different particle types at s to be

$$P_s^D = \frac{1}{2}\Big(B_s^x\big(A_v^1 + A_v^x\big) + B_s^{yx}\big(A_v^1 + A_v^{yx}\big) + B_s^{y^2x}\big(A_v^1 + A_v^{y^2x}\big)\Big), \tag{8.16}$$

$$P_s^E = \frac{1}{2}\Big(B_s^x\big(A_v^1 - A_v^x\big) + B_s^{yx}\big(A_v^1 - A_v^{yx}\big) + B_s^{y^2x}\big(A_v^1 - A_v^{y^2x}\big)\Big). \tag{8.17}$$

Finally, if the flux around p is C_y, then the projectors onto the different particle types at s are given by

$$P_s^F = \frac{1}{3}\Big(B_s^y\big(A_v^1 + A_v^y + A_v^{y^2}\big) + B_s^{y^2}\big(A_v^1 + A_v^y + A_v^{y^2}\big)\Big), \tag{8.18}$$

$$P_s^G = \frac{1}{3}\Big(B_s^y\big(A_v^1 + \omega A_v^y + \bar{\omega} A_v^{y^2}\big) + B_s^{y^2}\big(A_v^1 + \bar{\omega} A_v^y + \omega A_v^{y^2}\big)\Big), \tag{8.19}$$

$$P_s^H = \frac{1}{3}\Big(B_s^y\big(A_v^1 + \bar{\omega} A_v^y + \omega A_v^{y^2}\big) + B_s^{y^2}\big(A_v^1 + \omega A_v^y + \bar{\omega} A_v^{y^2}\big)\Big). \tag{8.20}$$

In principle, all the particles in the $D(S_3)$ quantum double model can be created, moved and fused by applying and/or deforming the corresponding ribbon operators, as is the case for any quantum double model. However, the actual implementation of the ribbon operators is highly non-trivial. A lot of work in this direction was done in Ref. [28], where the explicit operations to create and move pure fluxes and pure charges in the $D(S_3)$ quantum double model were thoroughly studied. In this reference a system based on an optical lattice was proposed as a possible experimental realization. More recently in Ref. [29], full protocols were given to create and move arbitrary anyons in the quantum double models, however without the specification of an explicit experimental realization.

In the following sections we perform a certain quantum computational operation using the $\{A, B, G\}$ submodel of the $D(S_3)$ anyon model. Let us therefore take a closer look at the anyons constituting this submodel. The other particles of the $D(S_3)$ particle spectrum can be treated in a similar way, with the details discussed in Refs. [28] and [29]. The B anyon is the simplest non-trivial particle of the $D(S_3)$ particle spectrum as it is the only non-trivial Abelian anyon. Similarly to the particles in the $D(\mathbb{Z}_2)$ quantum double model, the B anyon can be created and moved by applying single qudit unitaries to a path of qudits on the direct lattice. The explicit operator to create a pair of B anyons on two neighbouring vertices v, v' is given by the following unitary acting the direct triangle τ_{dir} with starting vertex v and ending vertex v':

$$F_{\tau_{\text{dir}}}^B = P_{\tau_{\text{dir}}}^1 - P_{\tau_{\text{dir}}}^y + P_{\tau_{\text{dir}}}^x - P_{\tau_{\text{dir}}}^{yx} + P_{\tau_{\text{dir}}}^{y^2} - P_{\tau_{\text{dir}}}^{y^2x}, \tag{8.21}$$

with the operation $P_{\tau_{\text{dir}}}^h$ defined in Eq. (4.18). Note that we omitted the parameters $\mathbf{u}$, $\mathbf{v}$ as there are no local degrees of freedom for the Abelian anyon

B. Furthermore, this operator does not depend on the orientation of the corresponding triangle, which is why we can label it by the single spin j that is contained in τ_{dir} and write

$$\begin{aligned} F_j^B = |1\rangle_j\langle 1| - |x\rangle_j\langle x| + |y\rangle_j\langle y| \\ - |yx\rangle_j\langle yx| + |y^2\rangle_j\langle y^2| - |y^2x\rangle_j\langle y^2x|. \end{aligned} \tag{8.22}$$

Finally, in the qubit-qutrit basis that was introduced above, this operator takes on the particularly simple form

$$F^B = \mathrm{Id}_3 \otimes \sigma^z. \tag{8.23}$$

The operator F_j^B can also be employed to move existing B anyons from one vertex to another. In contrast to this, the G particles are not only non-Abelian anyons but also dyons, which makes the corresponding creation and movement processes a lot more complicated. In order to create a pair of G anyons on neighbouring, non-overlapping sites we need to apply a ribbon operator $F_\rho^{G;\mathbf{u}}$ for arbitrary local flux degrees of freedom $\mathbf{u} = (i, i')$ and $\rho = \tau_{\mathrm{dual}}\tau_{\mathrm{dir}}$ for a composable dual and direct triangle. We may for example choose to trace out the local degrees of freedom by summing over all states with $i = i'$. Explicitly this corresponds to applying the ribbon operator

$$\begin{aligned} F_\rho^G := \sum_{i=1}^{2} F_\rho^{G;(i,i)} = \frac{1}{3}\big(L^y_{\tau_{\mathrm{dual}}}(P^1_{\tau_{\mathrm{dir}}} + \omega P^y_{\tau_{\mathrm{dir}}} + \bar\omega P^{y^2}_{\tau_{\mathrm{dir}}}) \\ + L^{y^2}_{\tau_{\mathrm{dual}}}(P^1_{\tau_{\mathrm{dir}}} + \bar\omega P^y_{\tau_{\mathrm{dir}}} + \omega P^{y^2}_{\tau_{\mathrm{dir}}})\big), \end{aligned} \tag{8.24}$$

Again we have omitted the parameter $\mathbf{v}$ since there are no local charge degrees of freedom for the G particles. The operations $L^g_{\tau_{\mathrm{dir}}}$ and $P^h_{\tau_{\mathrm{dir}}}$ were defined in Eqs. (4.18) and (4.18), respectively. Note that the resulting operation is not unitary, but it can be constructed using an adaptive procedure as explained in Ref. [29]. The same reference also describes how to extend arbitrary ribbon operators in order to move the corresponding particles around the lattice. How the required operations, in particular the ones involving projections, can actually be applied depends on the particular experimental realization.

To finish this summary of the $D(S_3)$ quantum double model let us quickly consider the gapped boundaries for this model. There are four subgroups of S_3 up to conjugation, which are the trivial subgroups $\{1\}$ and S_3, as well as $\{1, x\} \sim \mathbb{Z}_2$ and $\{1, y, y^2\} \sim \mathbb{Z}_3$. Except $\{1, x\}$ all of these subgroups are normal in S_3. Corresponding to these subgroups there are four different gapped boundaries for the $D(S_3)$ quantum double model. The particles that condense to the vacuum at each boundary can be determined using Eq. (5.10) in the case of $\{1, x\}$ or Eq. (5.11) for the normal subgroups. As for the $D(\mathbb{Z}_2)$ quantum double model we label each boundary by the anyons that get condensed to the vacuum. Again the trivial subgroup $\{1\}$ corresponds to the boundary where the pure charges get condensed, i.e. to the $A + B + 2C$ boundary. Note that the condensation multiplicity for the C anyon is two since the local subspace carried by the C anyon is two-dimensional, and any state within this space gets condensed to the vacuum at the boundary. The trivial subgroup S_3 corresponds to the boundary where the pure fluxes are condensed, i.e. to the $A + D + F$ boundary. For the normal subgroup $\{1, y, y^2\}$ the anyons that are condensed

to the vacuum are A, B and F with condensation multiplicity 2. Thus we call this boundary the $A + B + 2F$ boundary. Finally, for the subgroup $\{1, x\}$ the condensations to the vacuum are given by A, C, D and the corresponding boundary is thus called the $A + C + D$ boundary.

8.3 Computational power

It is a known fact that all the particles in the $D(S_3)$ anyon model carry finite images of the braid group [30], such that none of them allow universal quantum computation by braiding alone. However, if we allow certain additional operations, there are several ways to fault-tolerantly perform universal quantum computation with the $D(S_3)$ anyon model. It was shown in Ref. [31] that the $D(S_3)$ model is in principle capable of universal quantum computation using only pure fluxes and pure charges, given that we are able to provide a reservoir of ancillary flux states. In Ref. [27] universal quantum computation for a qutrit is proposed using certain measurements in the middle of a computation and ancillary states in addition to the topological operations. An explicit realization is not considered in both cases. However, Ref. [28] uses the ideas from Ref. [31] and explicitly describes the simulation of pure charges and fluxes in terms of the underlying spin lattice.

Because of its relative simplicity, the charge submodel $\{A, B, C\}$ has extensively been studied in the context of topological quantum computation. When studied on its own, this model is often called the Φ-Λ-model with the vacuum A denoted as 1, the Abelian anyon B denoted as Λ and the non-Abelian anyon C denoted as Φ. For consistency reasons, however, we stick to the notation introduced in Sec. 8.1. Even though the C particle is a non-Abelian anyon, its braiding behaviour is of the simplest possible kind, as its only effect on the fusion space is the effect required to describe the permutation of the corresponding anyons. In fact, it is shown in Ref. [32] that it is even possible to efficiently simulate the $\{A, B, C\}$ submodel of the $D(S_3)$ anyon model by the Abelian $D(\mathbb{Z}_6)$ quantum double model, which makes it clear that this submodel alone does not allow us to fully harness the non-Abelian structure of the $D(S_3)$ model. Nevertheless, the $\{A, B, C\}$ submodel can also be made universal by complementing the topological operations by a suitable set of non-topological operations, see Ref. [33].

In addition to the computational schemes that explicitly make use of the non-Abelian structure of $D(S_3)$ by storing logical information in the fusion spaces of non-Abelian anyons and processing it by braiding, it is also possible to generalize the hole encoding - that is typically used in Abelian models - to the non-Abelian case [15]. Moreover, it has been considered to introduce defects into the $D(S_3)$ quantum double model using combinations of boundaries based on different subgroups, see Ref. [16]. In both cases, the observed phenomena are remarkably richer than in the Abelian case.

9 Universal quantum computation using a hybrid quantum double model

We have stated in Sec. 7.3 that with the standard computational schemes for the $D(\mathbb{Z}_2)$ surface codes we can fault-tolerantly implement the full set of Clifford

group operations. In order to achieve universal quantum computation, we have to complement this set with one non-Clifford gate. In the following sections we show that this can be achieved using a hybrid quantum double model consisting of a $D(\mathbb{Z}_2)$ quantum double model separated from a $D(S_3)$ quantum double model by a suitable domain wall. In particular, we show in Sec. 9.1 that if we store a qubit in a suitable subspace of the fusion space of a quadruple of G anyons, it is possible to prepare a non-stabilizer state in the $D(S_3)$ phase. In Sec. 9.2 we discuss how this state can fault-tolerantly be transferred from the fusion space encoding to a hole-pair encoding. In Sec. 9.3 we then consider the different gapped domain walls between a $D(\mathbb{Z}_2)$ quantum double model and a $D(S_3)$ quantum double model. We determine the domain wall that best fits our purposes and explicitly write down the corresponding Hamiltonian. Sec. 9.4 discusses the exact operations that are needed to inject our non-stabilizer state - encoded in the anyonic occupancy of a hole-pair - into the $D(\mathbb{Z}_2)$ phase, while keeping superpositions of logical states protected at all times. Sec. 9.5 finally shows how this state can be used to perform a non-Clifford gate in the $D(\mathbb{Z}_2)$ phase, using only operations that can be performed fault-tolerantly.

9.1 A non-Clifford operation in the $D(S_3)$ quantum double model

In order to perform a non-Clifford operation in the $D(S_3)$ quantum double model we focus on the $\{A, B, G\}$ submodel of the $D(S_3)$ anyon model, where we exploit the non-Abelian braiding statistics of the G particle. In particular, let us consider four G particles with vacuum total fusion channel. We create one pair of G particles G_1, G_2 at the sites s_1, s_2 and a second pair G_3, G_4 at the sites s_3, s_4 such that all the particles are well separated from each other. Importantly, the numbers labelling the G particles are to be understood as referring to the sites that they live on and not to the particles themselves, as the individual anyons are indistinguishable. As discussed in Sec. 8.2, the explicit operations to create these pairs can be realized as following: We first create the pairs on neighbouring sites using the ribbon operator F^G_ρ, see Eq. (8.24). Subsequently, the particles can be moved apart following the protocol given in Ref. [29]. Using the notation that was introduced in Sec. 2.1 we can write the initial state of the four particles as $|G_1, G_2 \to A\rangle \otimes |G_3, G_4 \to A\rangle$, which we abbreviate as $|AA\rangle$. In total the fusion space V of four G particles created from the vacuum is 3-dimensional, as can easily be seen from the corresponding fusion rules in Table 8.3. Using similar abbreviated notations for all of the fusion channels, see Fig. 9.1(a), we can write $V = \text{span}(|AA\rangle, |BB\rangle, |GG\rangle)$. It would thus be natural to store a qutrit in this space. However, keeping in mind that we want to combine the computations performed in the $D(S_3)$ phase with computations that are performed in the $D(\mathbb{Z}_2)$ phase, we choose to encode a qubit in the subspace $\text{span}(|AA\rangle, |BB\rangle)$ by setting $|0\rangle_L := |AA\rangle$ and $|1\rangle_L := |BB\rangle$, while we do not use the third fusion channel. An arbitrary logical state can now be written as $|\psi\rangle_L = a|AA\rangle + b|BB\rangle$. Using ribbon operators, the logical basis states can explicitly be written as

$$|0\rangle_L = F^G_{\rho_{12}} F^G_{\rho_{34}} |GS\rangle, \qquad |1\rangle_L = F^B_{\rho_{23}} F^G_{\rho_{12}} F^G_{\rho_{34}} |GS\rangle, \tag{9.1}$$

where we have indexed the ribbons by their starting and ending sites and again have traced out the internal degrees of freedom. The logical X operator in

this encoding corresponds to the operator $F^B_{\rho_{23}}$, whereas the logical Z operator corresponds to a closed ribbon operator $K^A_\sigma - K^B_\sigma$, where σ encloses both G_1 and G_2, but no other excitations.

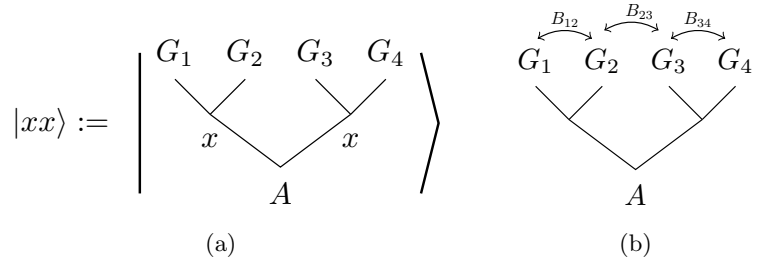

(a) (b)

Figure 9.1: (a) For $x \in \{A, B, G\}$ the basis states that span the fusion space of four G particles with vacuum total fusion channel are defined as indicated. (b) Graphical representation of the braiding matrices B_{12}, B_{23} and B_{34} acting on an arbitrary state in the fusion space $\text{span}(|AA\rangle, |BB\rangle, |GG\rangle)$. The arrows are used as an intuitive notation in order to indicate the single exchange of two particles.

The generators of the braid group representation carried by four G particles with vacuum total fusion channel can be found in Ref. [27] and are given by

$$B_{12} = B_{34} = e^{\frac{-i\pi}{9}} \begin{pmatrix} \omega^2 & 0 & 0 \\ 0 & -\omega^2 & 0 \\ 0 & 0 & \omega \end{pmatrix}, \tag{9.2}$$

$$B_{23} = e^{\frac{-i\pi}{9}} \begin{pmatrix} \frac{1}{2}\omega & -\frac{1}{2}\omega & \frac{1}{\sqrt{2}}\omega^2 \\ -\frac{1}{2}\omega & \frac{1}{2}\omega & \frac{1}{\sqrt{2}}\omega^2 \\ \frac{1}{\sqrt{2}}\omega^2 & \frac{1}{\sqrt{2}}\omega^2 & 0 \end{pmatrix} \tag{9.3}$$

in the basis $(|AA\rangle, |BB\rangle, |GG\rangle)$ and with $\omega = e^{\frac{2\pi i}{3}}$. They are represented pictorially in Fig. 9.1(b). Again these braidings can explicitly be performed in the spin lattice architecture by extending the ribbon operators of the corresponding particles. Since we are interested in operations on qubits, it is useful to note that the operation B^2_{23} is block diagonal and preserves the two-dimensional space $\text{span}(|AA\rangle, |BB\rangle)$ and its orthogonal complement $\text{span}(|GG\rangle)$. Explicitly we have

$$B^2_{23} = e^{\frac{-2i\pi}{9}} \begin{pmatrix} \cos\left(\frac{2\pi}{3}\right) & i\sin\left(\frac{2\pi}{3}\right) & 0 \\ i\sin\left(\frac{2\pi}{3}\right) & \cos\left(\frac{2\pi}{3}\right) & 0 \\ 0 & 0 & \omega \end{pmatrix}. \tag{9.4}$$

It is easy to check that this operation is not part of the Clifford group. Furthermore, by applying B^2_{23} to the state $|AA\rangle$, we can prepare the state

$$|\psi\rangle = \cos\left(\frac{2\pi}{3}\right)|AA\rangle + i\sin\left(\frac{2\pi}{3}\right)|BB\rangle, \tag{9.5}$$

ignoring a global phase factor. This state can be used to perform the non-Clifford operation

$$U = \begin{pmatrix} 1 & 0 \\ 0 & e^{\frac{2\pi i}{3}} \end{pmatrix} \tag{9.6}$$

on the space span($|AA\rangle, |BB\rangle$) following the arguments of Ref. [34], which we are going to summarize in Sec. 9.5. First, however, let us discuss the different steps that are needed in order to fault-tolerantly inject this state into the $D(\mathbb{Z}_2)$ phase.

9.2 Switching from the fusion space encoding to the hole encoding

The main approach to perform topological quantum computation in the $D(\mathbb{Z}_2)$ surface codes is to encode logical qubits in the anyonic occupancy of $1 + e$ or $1 + m$ holes. There exists no equivalent to the fusion space encoding that is typically used in non-Abelian models, as all the fusion spaces in Abelian models are trivial. In order to inject the state (9.5) into the $D(\mathbb{Z}_2)$ phase, we have to switch from the fusion space encoding to a hole-pair encoding. We now show how this can be achieved using a pair of $A+B+2C$ holes. Particular interest lies on the topological protection of the encoded information during all stages of the transfer. As in the previous subsection, we encode a qubit in the fusion space of a quadruple of G anyons with vacuum total fusion channel by setting $|0\rangle_L = |AA\rangle$ and $|1\rangle_L = |BB\rangle$. In order to distinguish between the fusion space encoding and the hole encoding, we will from now on use the subscript f for states corresponding to fusion channels and the subscript h for states corresponding to hole occupancies. An arbitrary logical state in the fusion space encoding can then be written as $|\psi\rangle_L = a|AA\rangle_f + b|BB\rangle_f$. We want to transfer this state to the hole-pair encoding given by the identification $|0\rangle_L = |AA\rangle_h$, $|1\rangle_L = |BB\rangle_h$ corresponding to the anyonic occupancy of two $A + B + 2C$ holes. The logical X operation in this encoding is given by F^B_ρ, where ρ is a ribbon connecting the two holes. The logical Z operation is given by $K^A_\sigma - K^B_\sigma$, where the closed ribbon σ encloses one of the holes completely, but no other excitations.

Consider the situation that is shown in Fig. 9.2(a), where we have a pair of G particles in an arbitrary state $|\psi\rangle_L = a|A\rangle_f + b|B\rangle_f$ and an empty $A+B+2C$ hole. Throughout this section we assume that the second pair of G particles and the second $A + B + 2C$ hole are both located far away, which means that errors tunneling a quasiparticle from one pair to the other are sufficiently unlikely. We thus are only concerned with logical Z errors. An operator that can cause such an error on the pair of G particles has to have support along a ribbon that encloses both G particles. Similarly, an operator that can cause such an error on the hole must have support on a ribbon that completely encloses the hole. Let us now move one of the G particles towards the hole until its charge part lies within the boundary of the hole, see Fig. 9.2(b). An operator that causes a logical Z error now has to enclose both the pair of G particles as well as the hole. If it was acting on the G particles alone, this operator would not commute with the single qudit terms acting on the edges inside the hole. As such, the A and B particles are now delocalized between both the pair of G particles and the vertices that are part of the hole. This situation becomes even clearer when we assume that the qudits inside the hole are removed from the code (with the plaquette stabilizers along the boundary of the hole modified accordingly). In this picture it is evident that the charge part of the G particle is delocalized inside the region of the hole as soon as it enters the hole. We can now do the same for the other G particle and move its charge part into the

hole as well, effectively fusing it with the charge part of the first G particle. This situation is shown in Fig. 9.2(c). Finally we annihilate the two G particles by fusing their flux parts, see Fig. 9.2(d). Note that the operations needed to move the G particles act locally on this pair of particles and in particular do not have support on a ribbon enclosing the hole. Repeating the same steps for the second pair of G particles and a second empty $A+B+2C$ hole leaves us with two $A+B+2C$ holes, which encode the logical state $|\psi\rangle_L = a|AA\rangle_h + b|BB\rangle_h$.

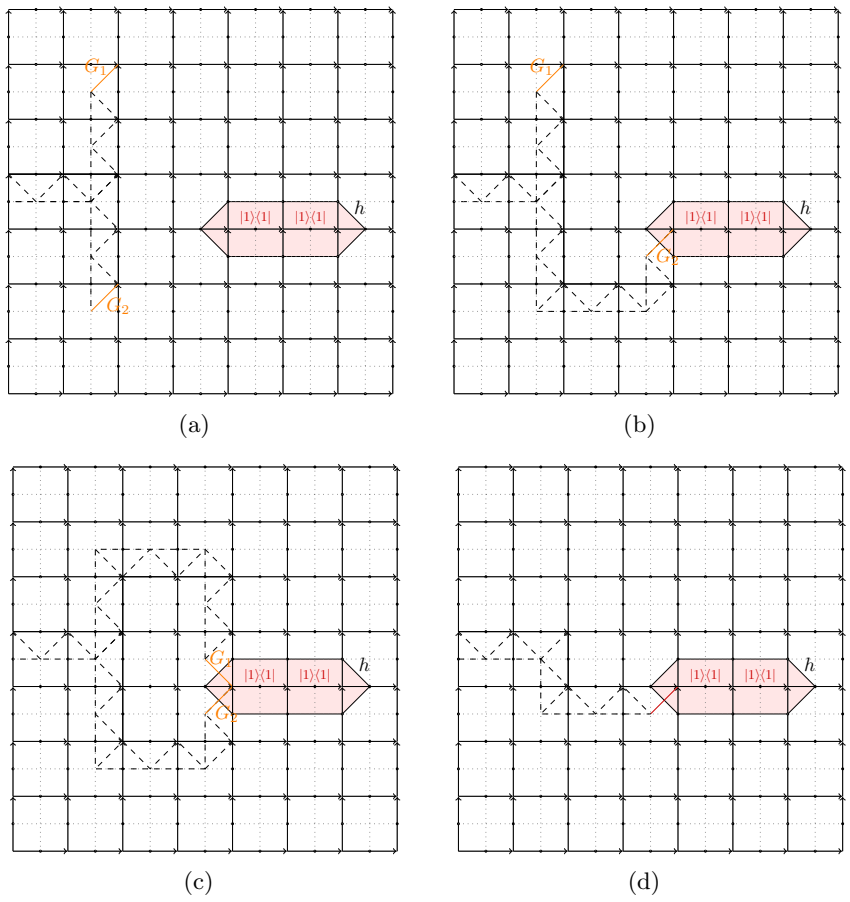

Figure 9.2: Transferring the anyonic occupancy of a pair of G particles to an $A+B+2C$ hole, mapping the state $a|A\rangle_f + b|B\rangle_f$ to the state $a|A\rangle_h + b|B\rangle_h$. (a) A pair of G particles in the state $|\psi\rangle_L = a|A\rangle_f + b|B\rangle_f$ and an $A+B+2C$ hole with vacuum anyonic occupancy, which corresponds to the state $|A\rangle_h$. (b) One of the G particles is moved until its charge part is located inside the hole. (c) The second G particle is moved into the hole as well and its charge part fused with the charge part of the first particle. (d) The flux parts of the two G particles are fused, removing the G particles from the lattice and leaving us with the hole in the state $|\psi\rangle_L = a|A\rangle_h + b|B\rangle_h$.

Also note that the projection onto the G fusion channel of the pair of G particles commutes with the single qudit terms acting inside the hole, as a G particle is not delocalized among the vertices comprising the hole. Similarly, any C particles that might accidentally enter the hole do not get delocalized among the G particles.

It would now be interesting to consider the reverse process, i.e. switching from the hole encoding to the fusion space encoding. However, this is not as easy as it might seem at first sight, as the fusion space encoding is inherently stronger than the hole-pair encoding. While the former is only accessible by truly non-local operations, such as explicitly bringing the two particles together, the logical state in our hole encoding is accessible by a LOCC protocol that simply measures the anyonic occupancy of all the vertices comprising the hole independently and then takes the parity of the result. The obvious analogue to the process described in Fig. 9.2 would be to create a pair of G anyons from the vacuum, fuse one of these particles with the hole that is in the logical state $|\psi\rangle_L = a|A\rangle_h + b|B\rangle_h$ and then contract the hole in order to completely transfer its anyonic occupancy to the pair of G particles. However, there is one major drawback to this procedure: Fusing a B particle with a G particle will in general cause a rotation in the local subspace carried by that G particle. Only the braiding operation leaves the local degrees of freedom invariant as long as the particles are well separated at all times; fusion with an additional particle, even though performing a rotation in the topologically protected space as well, may have an unwanted side effect that is locally detectable. In order to make this explicit, let us consider two different bases for the local subspace carried by a G particle that is located, say, at a site $s = (p, v)$. The local fluxes in C_y span this local subspace of this particle and we write $|y\rangle_{G,l}, |y^2\rangle_{G,l}$ for the corresponding basis states. Note that we have used the subscript G to indicate the particle type that we are concerned with and l to indicate that these states correspond to local degrees of freedom. Projectors onto these local basis states can be found from the general expression that was given in Eq. (4.37). They are simply given by $B_s^y P_s^G$, $B_s^{y^2} P_s^G$. Fusing a B particle with the G anyon corresponds to applying the operator F_j^B to the single spin located at an edge that connects the vertex v to an adjacent one. Obviously, this operation commutes with the projectors onto the local states as both are diagonal in the basis $\{|g\rangle | g \in G\}$. However, let us consider a different set of basis states for the internal degrees of freedom, namely the basis given by the states $|y\rangle_{G,l} + |y^2\rangle_{G,l}, |y\rangle_{G,l} - |y^2\rangle_{G,l}$. The corresponding projectors can be found from Eqs. (4.37) and (4.38). They are given by $(B_s^y + B_s^{y^2} + A_v^x B_s^y + A_v^x B_s^{y^2}) P_s^G$, $(B_s^y + B_s^{y^2} - A_v^x B_s^y - A_v^x B_s^{y^2}) P_s^G$ up to a constant factor. In this case, the single spin operation F_j^B flips the basis states as it anticommutes with the A_v^x terms. As such, the fusion with a B anyon leaves a local trace in the local subspace of the corresponding particle, which makes the information stored in the hole locally accessible when the hole is contracted. An approach that might be able to overcome this difficulty could be to use more than one pair of G particles. In particular one could imagine to transfer the anyonic occupancy of each vertex of the hole to a separate pair of G particles. By preparing all the G particles in a flux state of either $|y\rangle_{G,l}$ or $|y^2\rangle_{G,l}$ and assuming that local perturbations occur only with a very low probability, it might be possible to distill a single pair of G particles such that the anyonic occupancy of the hole is encoded non-locally in the fusion space of this single pair. We leave such considerations to a possible follow-up project. Note that if fusion with a B particle is used to perform a logical X on the qubit encoded in a quadruple of G anyons of known local state, the unwanted local rotation can in principle be reverted by applying a suitable correction operator from the set of operators given in Eq. (4.38) after every fusion. This was contemplated

in Ref. [33] in the case of C anyons, which show a similar behaviour upon the fusion with B anyons as the G anyons.

9.3 Gapped domain walls between the $D(S_3)$ phase and the $D(\mathbb{Z}_2)$ phase

As in Sec. 5.2, let us consider a lattice that is separated into two half-planes. The left half-plane is associated with the $D(\mathbb{Z}_2)$ quantum double model and the right half-plane is associated with the $D(S_3)$ quantum double model, see Fig. 9.3(a). The goal of this subsection is to define a domain wall separating the $D(S_3)$ and the $D(\mathbb{Z}_2)$ part of this hybrid model such that it is possible to transport logical information across this boundary, which in our case corresponds to qubits stored in the anyonic occupancy of a pair of $1+e$ holes in the $D(\mathbb{Z}_2)$ phase and in the anyonic occupancy of a pair of $A+B+2C$ holes in the $D(S_3)$ phase.

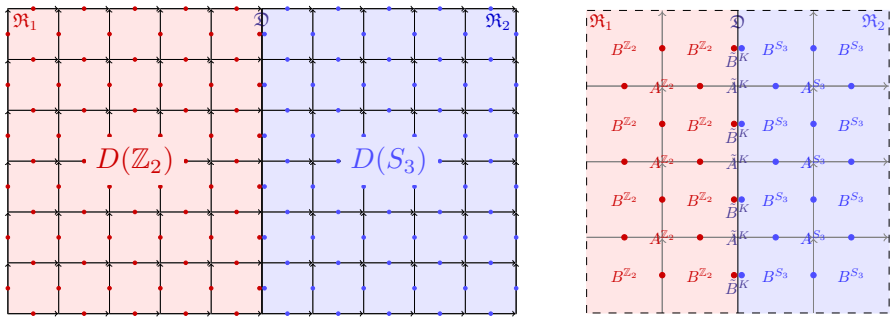

(a) (b)

Figure 9.3: (a) The lattice is divided into two half-planes. The left half-plane is associated with the $D(\mathbb{Z}_2)$ quantum double model and has qubits placed on each edge. These are indicated by red dots. The right half-plane is associated with the $D(S_3)$ quantum double model and thus has 6-level spins placed on each edge, which are shown as blue dots. Along the domain wall we have both a qubit and a 6-level spin placed on each edge. (b) The terms of the Hamiltonian near the domain wall. As argued in Sec. 5.2, we have special terms corresponding to a subgroup $K < \mathbb{Z}_2 \times S_3$ acting along the domain wall. The notations used here are defined in Secs. 5.1 and 5.2.

In order to determine the different gapped domain walls that are possible between the two phases, we employ the folding trick from Sec. 5.2. This means that we are interested in gapped boundaries of $D(\mathbb{Z}_2 \times S_3)$, which can be parametrized by subgroups $K < \mathbb{Z}_2 \times S_3$ and a 2-cocycle $\varphi \in H(K, \mathbb{C}^\times)$. There are 10 different subgroups of $\mathbb{Z}_2 \times S_3$ up to conjugation, which are listed in Table 9.1. Two of these subgroups additionally have a non-trivial 2-cocycle, which is why we count 12 different gapped domain walls between the $D(S_3)$ phase and the $D(\mathbb{Z}_2)$ phase in total. However, we restrict to considering the boundaries corresponding to trivial 2-cocycles. Note that except for K_4 and K_9 all the subgroups in Table 9.1 can be written as a direct product of a subgroup of $\mathbb{Z}_2$ and a subgroup of S_3, which means that the corresponding gapped domain walls can simply be identified as a boundary for the $D(\mathbb{Z}_2)$ quantum double model placed next to a boundary for the $D(S_3)$ quantum double model. In order to determine the

possible tunnelings of quasiparticles we consider the folded plane and determine which particles of the $D(\mathbb{Z}_2 \times S_3)$ particle spectrum (which are effectively pairs of particles of the $D(\mathbb{Z}_2)$ particle spectrum and the $D(S_3)$ particle spectrum) get condensed to the vacuum at each boundary. Table 9.2 lists the possible tunnelings that were obtained in this way for each of the 10 different gapped domain walls corresponding to trivial 2-cocycles. Note that our results coincide with those that were given in the appendix of Ref. [35].

	Subgroup	Order	Isomorphy class
K_1	$\{1\} \times \{1\}$	1	trivial
K_2	$\{1\} \times \{1, x\}$	2	$\mathbb{Z}_2$
K_3	$\{1, x\} \times \{1\}$	2	$\mathbb{Z}_2$
K_4	$\{(1,1), (x,x)\}$	2	$\mathbb{Z}_2$
K_5	$\{1\} \times \{1, y, y^2\}$	3	$\mathbb{Z}_3$
K_6	$\{1, x\} \times \{1, x\}$	4	$\mathbb{Z}_2 \times \mathbb{Z}_2$
K_7	$\{1, x\} \times \{1, y, y^2\}$	6	$\mathbb{Z}_6$
K_8	$\{1\} \times \{1, x, y, yx, y^2, y^2x\}$	6	S_3
K_9	$\{(1,1), (1,y), (1,y^2), (x,x), (x,yx), (x,y^2x)\}$	6	S_3
K_{10}	$\{1, x\} \times \{1, x, y, yx, y^2, y^2x\}$	12	$\mathbb{Z}_2 \times S_3$

Table 9.1: Subgroups of $\mathbb{Z}_2 \times S_3$. Note that K_4 and K_9 cannot be written as a direct product of a subgroup of $\mathbb{Z}_2$ and a subgroup of S_3.

For brevity let us use the intuitive notation $x \rightleftarrows y$ if the tunneling from an anyon x of the phase $D(\mathbb{Z}_2)$ to an anyon y of the phase $D(S_3)$ and vice versa is possible, and $x \not\rightleftarrows y$ if the tunneling is impossible. In order to turn a $1 + e$ hole into an $A + B + 2C$ hole when it crosses the domain wall, while mapping the logical state $|\psi\rangle_L = a|11\rangle + b|ee\rangle$ to the corresponding state $|\psi\rangle_L = a|AA\rangle + b|BB\rangle$, we are interested in a domain wall where

$$1 \rightleftarrows A, \qquad e \rightleftarrows B,$$

but

$$1 \not\rightleftarrows B, \qquad e \not\rightleftarrows A,$$
$$1 \not\rightleftarrows C, \qquad e \not\rightleftarrows C.$$

Importantly, note that these arrows are not intended to signify one-to-one correspondences, but simply state that the corresponding tunneling is possible in both directions.

	A	B	C	D	E	F	G	H
1	1	1	2					
e	1	1	2					
m								
ϵ								

(a) $K = K_1$

	A	B	C	D	E	F	G	H
1	1		1	1				
e	1		1	1				
m								
ϵ								

(b) $K = K_2$

	A	B	C	D	E	F	G	H
1	1	1	2					
e								
m	1	1	2					
ϵ								

(c) $K = K_3$

	A	B	C	D	E	F	G	H
1	1		1					
e		1	1					
m				1				
ϵ					1			

(d) $K = K_4$

	A	B	C	D	E	F	G	H
1	1	1				2		
e	1	1				2		
m								
ϵ								

(e) $K = K_5$

	A	B	C	D	E	F	G	H
1	1		1	1				
e								
m	1		1	1				
ϵ								

(f) $K = K_6$

	A	B	C	D	E	F	G	H
1	1	1				2		
e								
m	1	1				2		
ϵ								

(g) $K = K_7$

	A	B	C	D	E	F	G	H
1	1			1		1		
e	1			1		1		
m								
ϵ								

(h) $K = K_8$

	A	B	C	D	E	F	G	H
1	1					1		
e		1				1		
m				1				
ϵ					1			

(i) $K = K_9$

	A	B	C	D	E	F	G	H
1	1			1		1		
e								
m	1			1		1		
ϵ								

(j) $K = K_{10}$

Table 9.2: The allowed tunneling processes for the different gapped domain walls between the $D(\mathbb{Z}_2)$ phase and the $D(S_3)$ phase, corresponding to subgroups of $\mathbb{Z}_2 \times S_3$ and trivial 2-cocycles. A number in a given cell of the table indicates that the tunneling of the $D(\mathbb{Z}_2)$ particle specified in the leftmost column to the $D(S_3)$ particle specified in the top row is possible (with the corresponding multiplicity given by that number), whereas an empty cell corresponds to the tunneling multiplicity 0, i.e. an impossible tunneling. The labelling of the subgroups is defined in Table 9.1.

Looking at Table 9.2 we choose $K = K_9$ in order to realize our domain wall. The corresponding Hamiltonian can now easily be obtained from the theory that was presented in Sec. 5.2. We define the total Hamiltonian as

$$H = H^{S_3}(\mathfrak{R}_1) + H^{\mathbb{Z}_2}(\mathfrak{R}_2) + H^K(\mathfrak{D}), \tag{9.7}$$

where the different terms act on the vertices and plaquettes of the half-planes $\mathfrak{R}_1$ and $\mathfrak{R}_2$ and the domain wall $\mathfrak{D}$ as indicated in Fig. 9.3(b). Of particular interest are the operators that act on $\mathfrak{D}$. The vertex operators along the domain wall are given by

$$\begin{aligned}\tilde{A}_v^K = \frac{1}{6}(&\tilde{A}^1_{v_l} \otimes \tilde{A}^1_{v_r} + \tilde{A}^1_{v_l} \otimes \tilde{A}^y_{v_r} + \tilde{A}^1_{v_l} \otimes \tilde{A}^{y^2}_{v_r} \\ &+ \tilde{A}^x_{v_l} \otimes \tilde{A}^x_{v_r} + \tilde{A}^x_{v_l} \otimes \tilde{A}^{yx}_{v_r} + \tilde{A}^x_{v_l} \otimes \tilde{A}^{y^2x}_{v_r}),\end{aligned} \tag{9.8}$$

where the notations v_l, v_r for the left or right half of a vertex, respectively, were introduced in Sec. 5.2. Since K_9 cannot be written as a direct product of a subgroup of $\mathbb{Z}_2$ and a subgroup of S_3, the operator A_v^K cannot be written as a tensor product of an operator acting on v_l and an operator acting on v_r, a fact which is crucial in our construction. The plaquette operators B_p^K acting on a single pair consisting of a qubit and a 6-level spin explicitly read

$$\begin{aligned}\tilde{B}_p^K = &|1,1\rangle\langle 1,1| + |1,y\rangle\langle 1,y| + |1,y^2\rangle\langle 1,y^2| \\ &+ |x,x\rangle\langle x,x| + |x,yx\rangle\langle x,yx| + |y,y^2x\rangle\langle y,y^2x|.\end{aligned} \tag{9.9}$$

Therefore, if we focus on the case where we have no excitations on the domain wall plaquettes it may be preferable to replace the two spins located at each edge along the domain wall by a single 6-level spin and adjust the action of the operators that touch these spins appropriately. If we use the qubit-qutrit basis for the 6-level systems in the $D(S_3)$ part of the lattice and also for those on the domain wall, these modified operators take on a particularly nice form. In fact the modified plaquette operators $\hat{B}_p^{\mathbb{Z}_2}$ along the $D(\mathbb{Z}_2)$ side of the boundary keep their form but they now act on the qubit of the new 6-level system instead of acting on the qubit that was originally placed on the domain wall. The modified plaquette operators $\hat{B}_s^{S_3}$ along the $D(S_3)$ side of the boundary also keep their form, but act on the new 6-level system instead of acting on the 6-level system that was originally placed on the domain wall. The vertex operator $\tilde{A}_v^K$ now acts on three 6-level systems, one in the $D(S_3)$ part of the lattice and two on the domain wall, as well as on a single qubit in the $D(\mathbb{Z}_2)$ part of the lattice. The corresponding stabilizer circuit can conveniently be realized using the qubit-qutrit construction of the 6-level spins. In particular, we use the full vertex syndrome qudit as the control if a 6-level spin is the target, whereas we only use its qubit part as the control if the qubit is the target.

To provide an illustration of the theory developed so far, let us quickly look at the explicit operations in terms of the underlying spin lattice that are needed to realize the tunneling $e \rightleftarrows B$. For this consider Fig. 9.4. In the $D(\mathbb{Z}_2)$ phase the e particles are moved from one vertex to the next by applying single spin unitaries σ^z acting on the spin that is shared by these two vertices. Moving the e particle towards the domain wall, we arrive at the situation shown in Fig. 9.4(a), where the next vertex on the path is the domain wall vertex v_d. By applying σ^z to the next spin along the path we move the e particle from

the $D(\mathbb{Z}_2)$ phase to the domain wall, where it corresponds to the particle $(e, 1)$ living on the vertex $v_d = (v_l, v_r)$, see Fig. 9.4(b). This is signified by v_d now transforming according to the signed irreducible representation of S_3 instead of the trivial one. As is shown in Fig. 9.4(c), applying the operator F_B on the next spin in the $D(S_3)$ phase creates a pair of B anyons on v_r and its right adjacent vertex, with the pair (e, B) on (v_l, v_r) condensing to the vacuum by construction of the domain wall. In other words, v_d can now be seen to transform according to the trivial representation of S_3 again. We are then left with a single B anyon in the $D(S_3)$ phase, see Fig. 9.4(d), which can be moved as discussed in Sec. 8.2. The reverse tunneling can be realized in exactly the same way by reverting the steps described above. In the next subsection we generalize this to the process of moving a $1+e$ hole across the domain wall, where it becomes an $A+B+2C$ hole, and the logical state $|\psi\rangle_L = a|11\rangle + b|ee\rangle$ is mapped to $|\psi\rangle_L = a|AA\rangle + b|BB\rangle$.

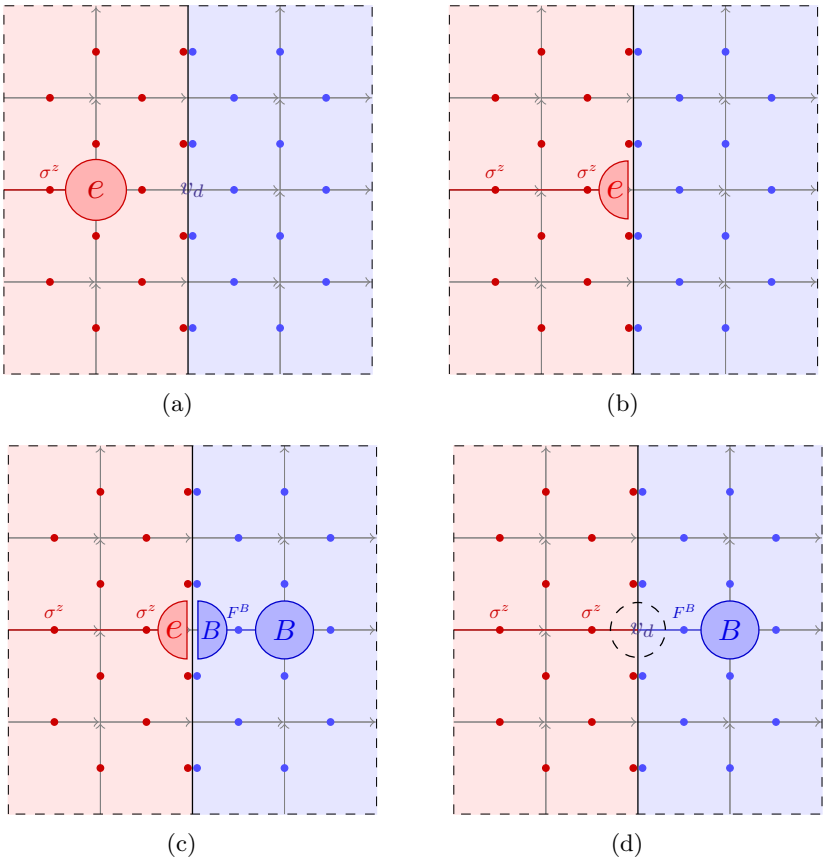

Figure 9.4: Tunneling an e particle from the $D(\mathbb{Z}_2)$ phase into the $D(S_3)$ phase. (a) An e particle in the $D(\mathbb{Z}_2)$ phase is moved towards the domain wall by applying single spin σ^z operations until the next vertex is the domain wall vertex v_d. (b) The e particle is moved to the domain wall vertex v_d by a σ^z operation, where it can be interpreted as residing on the left half v_l of the vertex $v_d = (v_l, v_r)$. (c) A pair of B anyons is created on the domain wall vertex v_d (or more specifically, on its right half v_r) and the adjacent vertex in the $D(S_3)$ phase. (d) Since the pair (e, B) on v_d condenses to the vacuum, we are left with a single B anyon in the $D(S_3)$ phase.

9.4 Transporting information across the domain wall

With the domain wall between the $D(\mathbb{Z}_2)$ phase and the $D(S_3)$ phase defined as in the previous subsection we can now look at the process of transporting logical information from one phase to the other. In the $D(S_3)$ phase we use the hole-pair encoding that was introduced in Sec. 9.2, and in the $D(\mathbb{Z}_2)$ phase we choose to encode information in a pair of $1+e$ holes by setting $|0\rangle_L := |11\rangle_h$, $|1\rangle_L := |ee\rangle_h$. We want to be able to move a $1+e$ hole in an arbitrary state $|\psi\rangle_L = a|1\rangle_h + b|e\rangle_h$ across the domain wall, where it turns into an $A+B+2C$ hole in the state $|\psi\rangle_L = a|A\rangle_h + b|B\rangle_h$, and vice versa. Again we assume that the second hole used to encode the logical qubit is situated sufficiently far away, such that we are only concerned with topological protection against logical Z errors. Consider a $1+e$ hole that is situated in the $D(\mathbb{Z}_2)$ part of the lattice. As long as the hole is large and well separated from any other hole the information stored in the anyonic occupancy of this hole is topologically protected. As discussed in Sec. 6, we can move this hole by subsequent contraction and expansion processes. In particular, the hole is enlarged by one cell width by measuring an adjacent spin in the basis $\{|g\rangle | g \in \mathbb{Z}_2\}$ and correcting the outcome if necessary. The hole is contracted by one cell width by measuring the anyonic occupancy of a vertex at the boundary of the hole, with a result corresponding to a non-trivial quasiparticle being corrected by moving the particle back into the hole. Suppose we move the $1+e$ hole towards the domain wall in this way until we arrive at the situation that is shown in Fig. 9.5(a). The next step in the movement implies enlarging the hole such that it encloses the domain wall vertex v_d, see Fig. 9.5(b). There are two things that we have to ensure: Firstly, the information stored in the $1+e$ hole must be properly delocalized not only in the $D(\mathbb{Z}_2)$ part of the hole but also in its $D(S_3)$ part. If this were not the case, the subsequent contraction of the $D(\mathbb{Z}_2)$ part of the hole would make the logical state $|\psi\rangle_L$ locally accessible. However, any operator causing a logical Z error at this stage of the transfer has to act on both the $D(\mathbb{Z}_2)$ part of the hole as well as v_r, as else this operator would not commute with the domain wall plaquette stabilizer $\tilde{B}_p^K$ and would therefore leave a local trace. In the presence of the Hamiltonian, such processes are suppressed by the energy gap. The situation becomes even clearer when we use the reduced domain wall construction described earlier, where the domain wall plaquettes are fixed in their ground state and implemented by 6-level systems instead of a combination of a qubit and a 6-level system. As such it is not possible to act on v_l and v_r separately from a hardware point of view. In either way, a logical operator causing a Z error to our state has to enclose both parts of the domain wall vertex v_d. Explicitly, the logical state of the hole is now given by the net e occupancy of the $D(\mathbb{Z}_2)$ part as well as the net occupancy of the vertex v_d in terms of pairs $(1, B)$ and (e, A), which are indistinguishable. Secondly, we have to make sure that this process does not corrupt the state $|\psi\rangle_L$ by tunnelings that mix the logical states. However, the way we defined the boundary ensures that this is not the case. Extending the hole further into the $D(S_3)$ phase by single spin measurements in the basis $\{|g\rangle | g \in S_3\}$ will cause the logical information to get delocalized further along the $D(S_3)$ part of the hole. When the $D(S_3)$ part of the hole is large enough we contract the $D(\mathbb{Z}_2)$ part by the usual protocol until we reach the situation that is shown in Fig. 9.5(c). Now we have to measure the vertex stabilizer corresponding to the domain wall vertex v_d in order to fully contract the $D(\mathbb{Z}_2)$ part of the hole. This

measurement can be done using the qubit-qutrit basis as described in Sec. 9.3. An outcome corresponding to a non-trivial quasiparticle is again corrected by moving that quasiparticle into the hole. Now we end up with an $A + B + 2C$ hole in the $D(S_3)$ part of the lattice as is shown in Fig. 9.5(d).

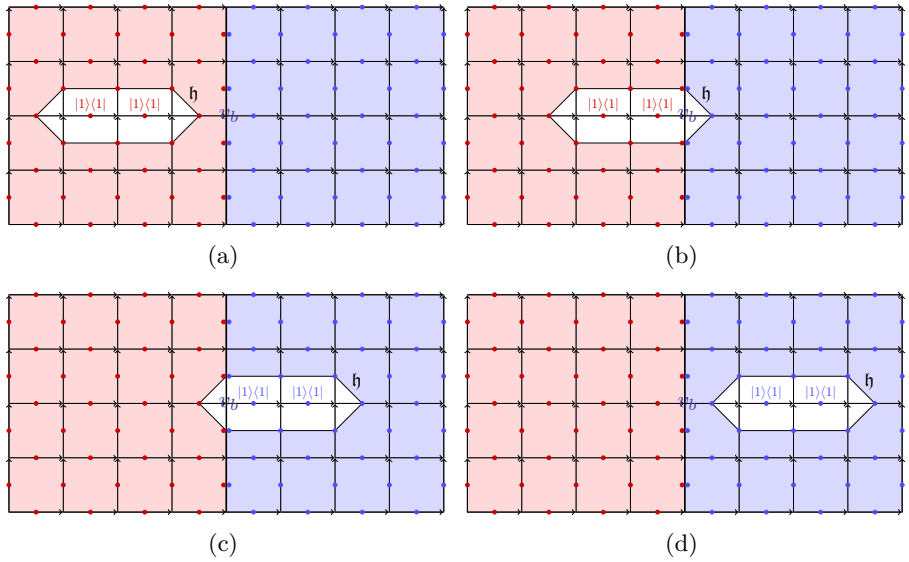

Figure 9.5: The process of moving a $1+e$ hole from the $D(\mathbb{Z}_2)$ phase across the domain wall, where it enters the $D(S_3)$ phase and becomes an $A+B+2C$ hole. Details on the explicit operations that are needed to perform the movement are given in the main text. (a) The hole is initially situated in the $D(\mathbb{Z}_2)$ part of the lattice. It can be moved by subsequent contraction and expansion processes as described earlier. (b) The hole is enlarged to enclose the domain wall vertex v_d. The anyonic occupancy of the hole is now given by the net occupancy of the $D(\mathbb{Z}_2)$ part of the hole and the occupancy of the vertex v_d. (c) The $D(\mathbb{Z}_2)$ part of the hole is contracted. The anyonic occupancy of the hole is now given by the net occupancy of the $D(S_3)$ part of the hole and the occupancy of the vertex v_d. (d) The vertex v_d is measured in order to fully contract the $D(\mathbb{Z}_2)$ part of the hole. If an anyon is measured to reside on this vertex (and no other anyon of this kind is located at a close position), it is moved into the hole in order to preserve the corresponding logical state.

The reverse process can be realized by reverting the steps (a) to (d) shown in Fig. 9.5 and arguing in the same way as above. However, additional interest should be paid to the fact that the measurement of v_d in the final contraction step can yield an outcome corresponding to a pair $(1, C)$ or (e, C) located on v_d. Again let us emphasize that these two pairs are indistinguishable. Since the C anyons cannot enter the $D(\mathbb{Z}_2)$ phase it might not be clear how to correct for this measurement outcome. However, recall that we are only interested in moving $A+B+2C$ holes across the boundary whose anyonic occupancy is given by a state $|\psi\rangle_L \in \mathrm{span}(|AA\rangle_h, |BB\rangle_h)$. This means that any C particle that might reside on the boundary vertex v_d during the contraction process from the situation shown in Fig. 9.5(b) to the situation shown in Fig. 9.5(a) must have entered the hole as the consequence of an error in the $D(S_3)$ part of the hybrid model, and another stray C anyon (or a collection of stray anyons with total

fusion channel C) has to be located somewhere in the $D(S_3)$ phase. Since we assume the probability for such errors to be small and we correct for errors on a regular basis, this C anyon will be located somewhere near the vertex v_d. We now need to fuse this C anyon with the one residing at v_d. This is crucial since there might be an e or B anyon hidden within the C anyon at v_d, which we need to recover and fuse with the hole in order to preserve its logical state.

9.5 Completing the gate set

This subsection is just a short summary of a particular result presented in Ref. [34]. With the tools that were developed in Secs. 9.1-9.4 it is possible to prepare the state $|\psi\rangle_L = \cos\left(\frac{2\pi}{3}\right)|AA\rangle_f + i\,\sin\left(\frac{2\pi}{3}\right)|BB\rangle_f$ in the $D(S_3)$ phase, transform this state into $|\psi\rangle_L = \cos\left(\frac{2\pi}{3}\right)|AA\rangle_h + i\,\sin\left(\frac{2\pi}{3}\right)|BB\rangle_h$ and finally inject the state into the $D(\mathbb{Z}_2)$ phase, where it emerges as

$$|\psi\rangle_L = \cos\left(\frac{2\pi}{3}\right)|11\rangle_h + i\,\sin\left(\frac{2\pi}{3}\right)|ee\rangle_h. \tag{9.10}$$

The notations for the computational basis states were introduced in the previous subsections. In particular, we identify the logical basis in the $D(\mathbb{Z}_2)$ phase as $|0\rangle_L = |11\rangle_h$, $|1\rangle_L = |ee\rangle_h$. However, in order to avoid cluttering the notation, we omit the subscript L in the following argument. Let us now briefly summarize how many copies of the state $|\psi\rangle$ can be used in order to perform the non-Clifford unitary

$$U = \begin{pmatrix} 1 & 0 \\ 0 & e^{\frac{2\pi i}{3}} \end{pmatrix} \tag{9.11}$$

on a logical qubit given that we are able to fault-tolerantly perform the following operations: i) initialize logical qubits in the state $|0\rangle$, ii) perform arbitrary Clifford operations on logical qubits and iii) measure logical qubits in any Pauli basis. All of these assumptions are justified in a standard implementation of the $D(\mathbb{Z}_2)$ surface code using the hole-pair encoding. The qubit corresponding to the state $|\psi\rangle$ is from now on going to be referred to as the ancillary qubit. The unitary operation U can now be performed on a qubit in the arbitrary state $|\varphi\rangle = a|0\rangle + b|1\rangle$, which we are going to call the computational qubit, by the following steps:

1. Apply a Hadamard gate to the state $|\psi\rangle$ in order to obtain the state

$$|\psi'\rangle = H|\psi\rangle = \frac{e^{\frac{2\pi i}{3}}}{\sqrt{2}}\left(|0\rangle + e^{\frac{2\pi i}{3}}|1\rangle\right). \tag{9.12}$$

   By ignoring the global phase this is equivalent to the state

$$|\psi'\rangle = \frac{1}{\sqrt{2}}\left(|0\rangle + e^{\frac{2\pi i}{3}}|1\rangle\right). \tag{9.13}$$

2. Prepare the state $|\Psi_0\rangle = |\varphi\rangle \otimes |\psi'\rangle$.

3. Measure $\sigma^z \otimes \sigma^z$. The possible measurement outcomes are $+1$ and -1, both occurring with probability $1/2$. If the outcome is $+1$, we are left with the state

$$|\Psi_1^+\rangle = a|00\rangle + be^{\frac{2\pi i}{3}}|11\rangle. \tag{9.14}$$

If the measurement outcome is -1, the resulting state is

$$|\Psi_1^-\rangle = ae^{\frac{2\pi i}{3}}|01\rangle + b|10\rangle. \tag{9.15}$$

4. Apply a CNOT gate with the computational qubit as the control and the ancillary qubit as the target. The resulting states are

$$|\Psi_2^+\rangle = \left(a|0\rangle + be^{\frac{2\pi i}{3}}|1\rangle\right) \otimes |0\rangle, \tag{9.16}$$

$$|\Psi_2^-\rangle = \left(ae^{\frac{2\pi i}{3}}|0\rangle + b|1\rangle\right) \otimes |1\rangle, \tag{9.17}$$

which leaves the ancillary qubit disentangled from the system.

5. Discard the ancillary qubit. The net effect of this procedure is thus the application of either U or U' to the computational qubit, with

$$U = \begin{pmatrix} 1 & 0 \\ 0 & e^{\frac{2\pi i}{3}} \end{pmatrix}, \qquad U' = \begin{pmatrix} 1 & 0 \\ 0 & e^{-\frac{2\pi i}{3}} \end{pmatrix}. \tag{9.18}$$

6. By repeating this procedure for many copies of the ancillary state $|\psi\rangle$ (which can be easily prepared as discussed in the previous subsections), we will eventually succeed in realizing the gate U, and the probability that we require more than N steps in order to achieve this decreases exponentially with N. For more details on this argument, the reader is referred to the original paper [34].

Finally, it is shown in Ref. [36] that the full Clifford group supplemented with a single arbitrary non-Clifford gate allows for universal quantum computation.

10 Conclusion

There are several known ways in which the full set of Clifford operations can be fault-tolerantly performed in the $D(\mathbb{Z}_2)$ surface codes. The usual way to complete this set such that we are able to perform universal quantum computation is by magic state distillation. In this thesis we have discussed an alternative approach to complement the gate set of the $D(\mathbb{Z}_2)$ surface codes. We have considered a hybrid quantum double model, where one part of the lattice is associated with the quantum double model based on the group $\mathbb{Z}_2$ and another part is associated with the quantum double model based on the non-Abelian group S_3. In particular we have proposed an explicit Hamiltonian realization of a gapped domain wall between the $D(\mathbb{Z}_2)$ phase and the $D(S_3)$ phase using the folding idea. We have described how a non-stabilizer state can be prepared in the $D(S_3)$ phase and have given the explicit operations that are needed to inject this state into the $D(\mathbb{Z}_2)$ phase while preserving the logical information it contains. Several copies of this state can then be used to perform a non-Clifford operation in the $D(\mathbb{Z}_2)$ phase. This provides us with an interesting alternative to magic state distillation. While we have focused on an explicit example, it would be interesting to study the transport of information between topological phases based on different quantum double models systematically in a more abstract context. In general we believe that the concept of hybrid quantum double

models provides an interesting and very flexible platform to find novel schemes for universal quantum computation.

Furthermore, we have considered the realization of non-Abelian quantum double models, in particular the $D(S_3)$ model, using local stabilizer circuits. We have given circuits that perform plaquette and vertex measurements in a similar way as in the $D(\mathbb{Z}_2)$ case, and have interpreted the syndrome information that can be obtained in such a way. However, we have not dealt with explicit error correction protocols.

Apart from this we have reviewed several aspects of the theory of quantum double models and the underlying abstract anyon models in a way that should be accessible to a broad audience. While this review is of course in no way complete and lacks any mathematical rigour, our goal was to give a clear outline of the general concepts allowing the reader to follow the original references more easily.

References

[1] A.Yu. Kitaev. Fault-tolerant quantum computation by anyons. *Annals of Physics*, 303(1):2–30, 2003.

[2] Michael A. Nielsen and Isaac L. Chuang. *Quantum Computation and Quantum Information*. Cambridge University Press, 2000.

[3] John Preskill. Lecture Notes for Physics 219: Quantum Computation. 2004.

[4] Jiannis K. Pachos. Introduction to Topological Quantum Computation. 2012.

[5] Michael H. Freedman, Michael J. Larsen, and Zhenghan Wang. The two-eigenvalue problem and density of Jones representation of braid groups. *Communications in Mathematical Physics*, 228(1):177–199, 2002.

[6] F. Alexander Bais, Peter van Driel, and Mark de Wild Propitius. Quantum symmetries in discrete gauge theories. *Physics Letters B*, 280(1-2):63–70, 1992.

[7] Mark De Wild Propitius. Topological interactions in broken gauge theories. *arXiv*, (september):168, 1995.

[8] Mark De Wild Propitius and F. Alexander Bais. Discrete gauge theories. *arXiv*, (280):2, 1995.

[9] Ville Lahtinen. Anyons, Quantum Double Symmetry and Topological Quantum Computation. page 42, 2006.

[10] Vladimir Drinfeld. Quantum Groups. *International Congress of Mathematicians*, pages 798–820, 1987.

[11] Daniel Gottesman. Class of quantum error-correcting codes saturating the quantum Hamming bound. *Physical Review A*, 54(3):1862–1868, sep 1996.

[12] H. Bombin and M. A. Martin-Delgado. Family of non-Abelian Kitaev models on a lattice: Topological condensation and confinement. *Physical Review B - Condensed Matter and Materials Physics*, 78(11):1–28, 2008.

[13] Sergey B. Bravyi and Alexei Yu. Kitaev. Quantum codes on a lattice with boundary. *arXiv*, (96):6, 1998.

[14] Salman Beigi, Peter W. Shor, and Daniel Whalen. The Quantum Double Model with Boundary: Condensations and Symmetries. *Communications in Mathematical Physics*, 306(3):663–694, 2011.

[15] Iris Cong, Meng Cheng, and Zhenghan Wang. Topological Quantum Computation with Gapped Boundaries. 2016.

[16] Iris Cong, Meng Cheng, and Zhenghan Wang. On Defects Between Gapped Boundaries in Two-Dimensional Topological Phases of Matter. pages 1–21, 2017.

[17] Eric Dennis, Alexei Kitaev, Andrew Landahl, and John Preskill. Topological quantum memory. *Journal of Mathematical Physics*, 43(9):4452–4505, 2002.

[18] Austin G. Fowler, Ashley M. Stephens, and Peter Groszkowski. High-threshold universal quantum computation on the surface code. *Physical Review A - Atomic, Molecular, and Optical Physics*, 80(5):1–18, 2009.

[19] Austin G. Fowler, Matteo Mariantoni, John M. Martinis, and Andrew N. Cleland. Surface codes: Towards practical large-scale quantum computation. *Physical Review A - Atomic, Molecular, and Optical Physics*, 86(3), 2012.

[20] Barbara M. Terhal. Quantum error correction for quantum memories. *Reviews of Modern Physics*, 87(2):307–346, 2015.

[21] James R. Wootton, Jan Burri, Sofyan Iblisdir, and Daniel Loss. Error correction for non-Abelian topological quantum computation. *Physical Review X*, 4(1):1–15, 2014.

[22] Adrian Hutter, Daniel Loss, and James R. Wootton. Improved HDRG decoders for qudit and non-Abelian quantum error correction. *New Journal of Physics*, 17:1–17, 2015.

[23] Cristopher Moore, Daniel Rockmore, and Alexander Russell. Generic Quantum Fourier Transforms. 2(4):707–723, 2003.

[24] Daniel Gottesman. Stabilizer Codes and Quantum Error Correction. 2008, may 1997.

[25] Clare Horsman, Austin G. Fowler, Simon Devitt, and Rodney Van Meter. Surface code quantum computing by lattice surgery. *New Journal of Physics*, 14, 2012.

[26] Benjamin J. Brown, Katharina Laubscher, Markus S. Kesselring, and James R. Wootton. Poking holes and cutting corners to achieve Clifford gates with the surface code. pages 1–18, 2016.

[27] Shawn X. Cui, Seung-Moon Hong, and Zhenghan Wang. Universal quantum computation with weakly integral anyons. *Journal of Mathematical Physics*, 56(3):1–44, jan 2014.

[28] G. K. Brennen, M. Aguado, and J. I. Cirac. Simulations of quantum double models. *New Journal of Physics*, 11, 2009.

[29] Xi Wang Luo, Yong Jian Han, Guang Can Guo, Xingxiang Zhou, and Zheng Wei Zhou. Simulation of non-Abelian anyons using ribbon operators connected to a common base site. *Physical Review A - Atomic, Molecular, and Optical Physics*, 84(5):1–11, 2011.

[30] Pavel Etingof, Eric C. Rowell, and Sarah Witherspoon. Braid group representations from twisted quantum doubles of finite groups. *Arxiv preprint*, pages 1–8, 2007.

[31] Carlos Mochon. Anyon computers with smaller groups. *Physical Review A - Atomic, Molecular, and Optical Physics*, 69(3):032306–1, 2004.

[32] James R. Wootton, Ville Lahtinen, Zhenghan Wang, and Jiannis K. Pachos. Non-abelian statistics from an abelian model. *Phys. Rev. B.*, 78:16102, 2008.

[33] James R. Wootton, Ville Lahtinen, and Jiannis K. Pachos. Universal quantum computation with a non-Abelian topological memory. *Lecture Notes in Computer Science (including subseries Lecture Notes in Artificial Intelligence and Lecture Notes in Bioinformatics)*, 5906 LNCS:56–65, 2009.

[34] Sergey Bravyi and Alexei Kitaev. Universal quantum computation with ideal Clifford gates and noisy ancillas. *Physical Review A*, 71(2):022316, feb 2005.

[35] Tian Lan, Juven C. Wang, and Xiao Gang Wen. Gapped domain walls, gapped boundaries, and topological degeneracy. *Physical Review Letters*, 114(7):1–5, 2015.

[36] Gabriele Nebe, E. M. Rains, and N. J A Sloane. The Invariants of the Clifford Groups. *Designs, Codes, and Cryptography*, 24(1):99–122, 2001.